

## 2001 MARS ODYSSEY PROJECT REPORT

**David A. Spencer, Odyssey Mission Manager**  
**Roger G. Gibbs, Odyssey Project Manager**  
**Robert A. Mase, Odyssey Navigation Team Lead**  
**Jeffrey J. Plaut, Odyssey Deputy Project Scientist**  
**Ronald S. Saunders, Odyssey Project Scientist**  
**Jet Propulsion Laboratory**  
**California Institute of Technology**  
**Pasadena, California**

### Abstract

The Mars Odyssey orbiter was launched on April 7, 2001, and arrived at Mars on October 24, 2001. The orbiter carries scientific instruments that will determine surface elemental composition, mineralogy and morphology, and measure the Mars radiation environment from orbit. In addition, the orbiter will serve as a data relay for future surface missions. This paper will present an overview of the Odyssey project, including the key elements of the spacecraft design, mission design and navigation, mission operations, and the science approach. The project's risk management process will be described. Initial findings of the science team will be summarized.

### Introduction

The Mars Odyssey Project is the latest in an ongoing series of robotic missions to Mars within NASA's Mars Exploration Program. The Program goals include the global observation of Mars, to enable understanding of the Mars climatic and geologic history, including the search for liquid water and the evidence of prior or extant life. The Odyssey orbiter carries scientific payloads that will determine surface elemental composition, mineralogy

and morphology, and measure the Mars radiation environment from orbit. In addition, the orbiter will serve as a data relay for future landed assets. Odyssey was designed and developed through a partnership between the Jet Propulsion Laboratory in Pasadena, California, and Lockheed Martin Astronautics in Denver, Colorado.

The Odyssey spacecraft was launched from Kennedy Space Center on April 7, 2001, and successfully captured into orbit about Mars on October 24, 2001. Following 76 days of aerobraking, a series of five propulsive maneuvers were performed to attain the near-circular science orbit. The science mission formally began on February 19, 2002. The prime science mission lasts for 917 days, and will be completed on August 24, 2004.

The primary science objectives are the following:

- Globally map the elemental composition of the Mars surface.
- Determine the abundance of Hydrogen in the shallow subsurface.
- Acquire high spatial and spectral resolution of the surface mineralogy.
- Provide information on the morphology of the surface.

- Assess the Mars radiation environment.
- Provide data for evaluation of future landing sites.

The mission success criteria as stated in the *Project Policies Document*<sup>1</sup> are expressed as “primary” and “full” mission success

criteria. The mission success criteria are shown in Table 1. The strategy for meeting the project mission objectives is described in the *Mission Plan*<sup>2,3</sup>. The detailed implementation plan is given in the *Baseline Reference Mission*<sup>4</sup> document.

Table 1. Mission Success Criteria

Full Mission Success	Primary Mission Success
<ul style="list-style-type: none"> <li>• Carry out a global survey of Mars from the planned science orbit for one Mars year.</li> <li>• Collect 75% of the planned mission science data from each of the orbiter science instrument complements.</li> <li>• Provide communications relay for surface elements from the U.S. and other spacefaring nations for two Mars years after achieving the science orbit.</li> <li>• Archive the acquired science data in the Planetary Data System within 6 months of acquisition.</li> </ul>	<ul style="list-style-type: none"> <li>• Acquire 25% of the planned mission science data from Mars orbit for two out of three of the orbiter science instrument complements.</li> <li>• Archive the acquired science data in the Planetary Data System.</li> </ul>

### Spacecraft Development

The Jet Propulsion Laboratory teamed with its industrial partner, Lockheed Martin Astronautics, to design, build and test the Odyssey orbiter. The design drew heavily from the heritage designs of the Mars Climate Orbiter and Stardust spacecraft.

### System Description

The system block diagram is shown in Figure 1. The subsystems which comprise the Odyssey are: command and data handling, electrical power, guidance navigation and control, mechanisms, propulsion, science payload, flight software and fault protection, structure and harness, telecommunication, and thermal control.

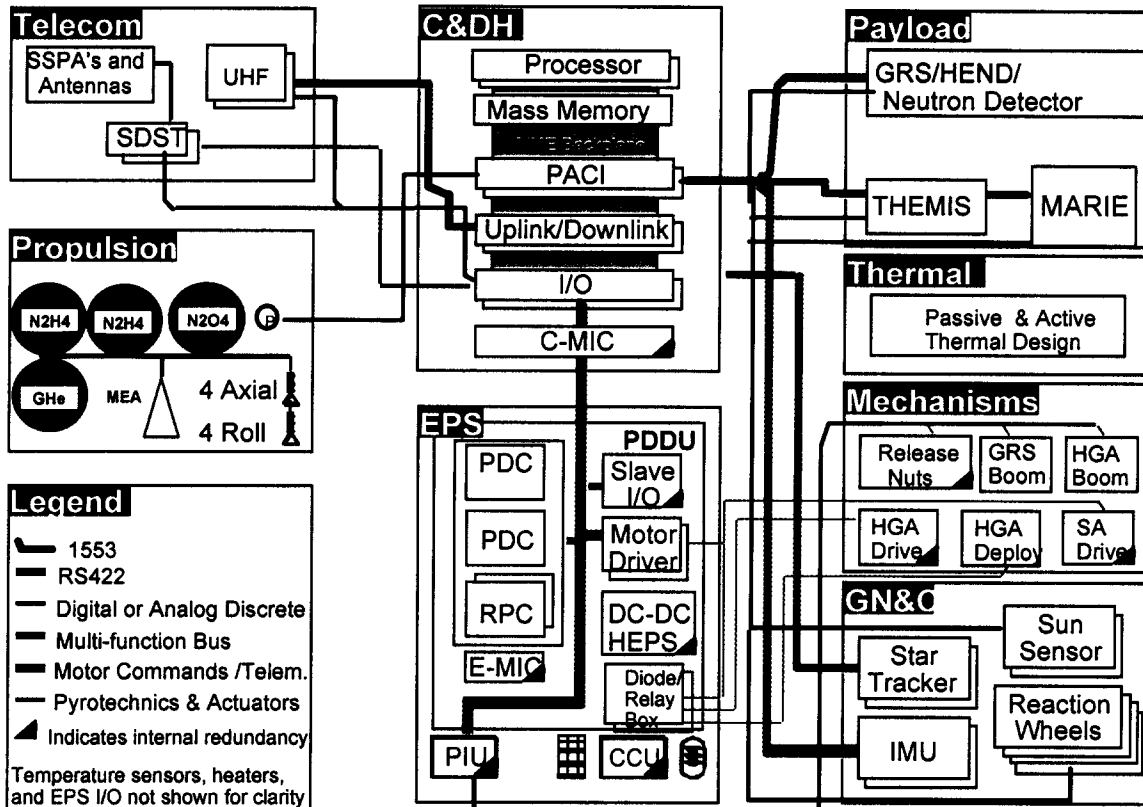


Figure 1. System Block Diagram

### Command and Data Handling

The command and data handling (C&DH) subsystem receives data files and commands from the ground operators via the telecommunication subsystem, stores and executes sequenced commands and autonomously generated commands, collects

telemetry and sensor data from the guidance, navigation, and control sensors and provides control of the reaction wheels and thrusters, collects sensor data from the science instruments, and formats data for transmission to the ground operators via the telecommunication subsystem.

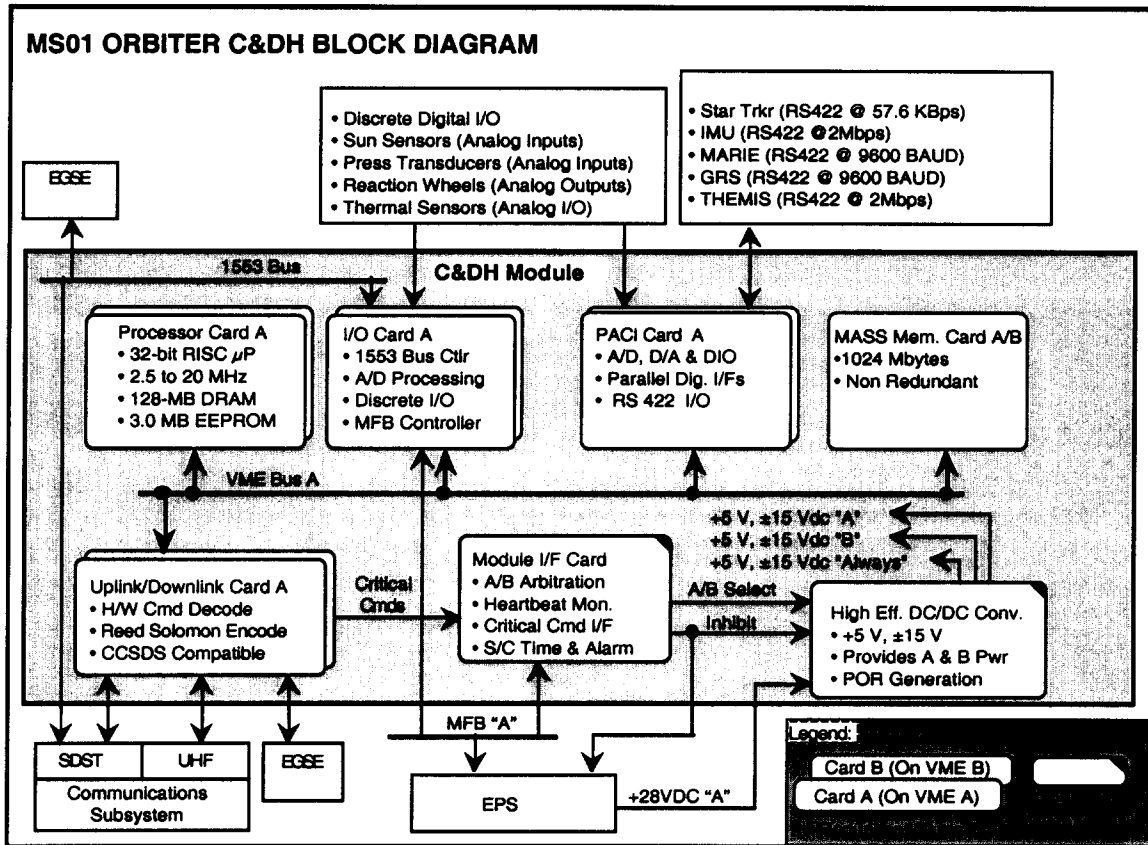


Figure 2. Command and Data Handling Block Diagram

There are seven modules in the C&DH. The processor card contains a RAD6000 processor, 128 megabytes of random access memory and 3 megabytes of non-volatile memory. There is a redundant processor card.

The input/output card collects analog data from sensors distributed on the spacecraft and converts this signal to a data word(s); provides the control of the Mil-Spec 1553 and multi-function data busses; and collects discrete (binary) telemetry. The input/output card is redundant.

The payload and attitude control interface card collects telemetry from and provides commands to the science instruments and the guidance, navigation, and control sensors and actuators. The payload and attitude control interface card is redundant.

The uplink/downlink card provides the interface to the telecommunication subsystem, both x-band and UHF. The uplink/downlink card provides command decoding on data received from the ground operators and encodes data transmitted. The uplink/downlink card is redundant.

The mass memory card stores data for later transmission to ground operators. The data volume capability is 1024 Mbytes.

The module interface card arbitrates if there is contention between the two processors, provides a critical oversight function on the processor (the "heartbeat monitor"), and maintains the master spacecraft clock and status of the mission phase.

**Electrical Power**

The electrical power subsystem (EPS) generates, stores, and distributes the electrical power used on Odyssey. Electrical power is generated by the 7.4 square meter solar array. This solar array is comprised of gallium arsenide solar cells bonded to three composite panels. At Mars,

the solar array is capable of producing approximately 540-780 watts of electrical power, depending on solar distance and incidence angle. When illuminated by the sun the solar array provides the electrical power requirements of the Odyssey and keeps the battery fully charged.

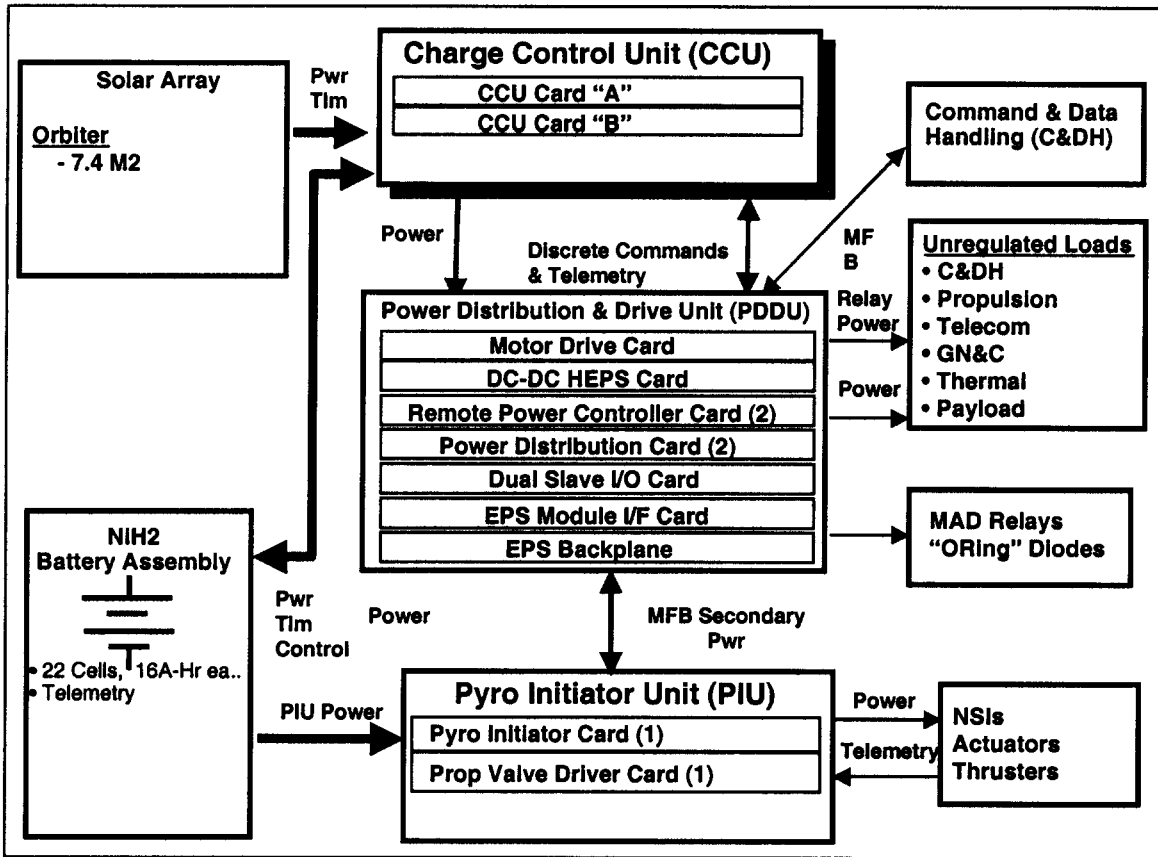


Figure 3. Electrical Power Subsystem Block Diagram

A 22 cell, 16 amp-hr nickel-hydrogen battery provides the power requirements when the solar array is not generating sufficient electrical energy, such as when Mars eclipses the sun in orbit, or the spacecraft must change orientations for a thruster maneuver.

The charge control unit controls the energy provided to the battery according to the

condition of the battery as monitored by the voltage, temperature, and pressure of the battery. The charge control unit is redundant.

The power distribution and drive unit provides electrical power switching and distribution, motor control drive for actuators, and regulated bus voltage via high efficiency dc/dc converters. The power

distribution and drive unit is redundant. The motor and drive unit provides relays and diodes to ensure redundant capability even in the presence of electrical shorts in the actuation devices.

The pyrotechnic initiator unit actuates the release and activation devices (separator nuts, thermal wax actuators, and NASA standard initiators) and controls the propulsion engine valves. The pyrotechnic initiator unit is redundant.

### **Guidance Navigation and Control**

The guidance navigation and control subsystem maintains knowledge of the orientation of the spacecraft relative to an inertial reference coordinate system, maintains the knowledge of the positions of the Earth, sun, and Mars, controls the

spacecraft body, solar array normal vector, high gain antenna centerline, and science instrument boresights either individually or collectively to track stationary or moving vectors (example: control the THEMIS boresight to track Mars nadir, the solar array normal vector to track the sun, and the high gain antenna boresight to track Earth), controls the propulsion subsystem to impart velocity changes or to unload the momentum energy in the reaction wheels.

The sun sensors provide pointing data on the position of the sun. The star tracker provides position and illumination magnitude data of the star field. The inertia measurement unit uses ring laser diode gyros and an accelerometer to provide spin and acceleration rates. These sensors are redundant.

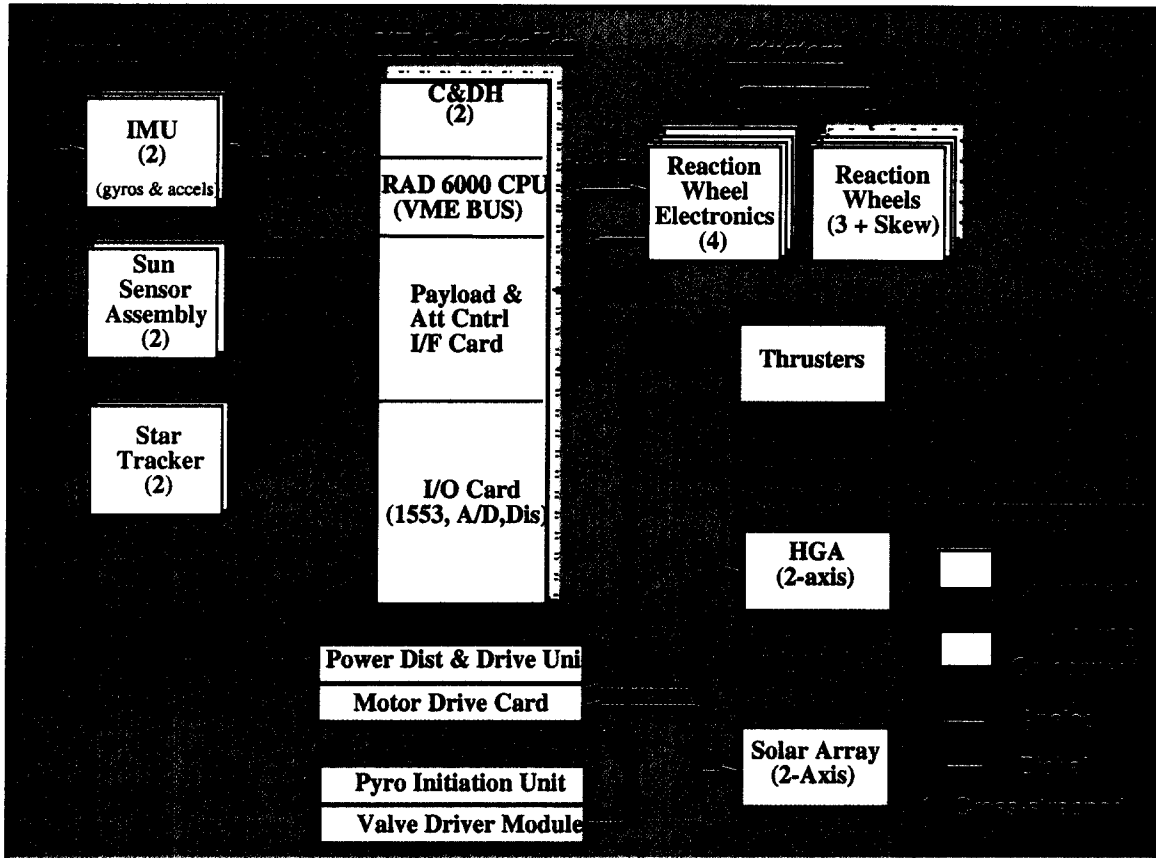


Figure 4. Guidance Navigation and Control Block Diagram

The control algorithms, hosted in the command and data handling subsystem, process these sensor inputs and provide control data for the actuators.

The reaction wheels provide three axis roll control of the spacecraft. The thrusters, part of the propulsion subsystem, provide capability to control roll orientation in pitch, yaw, and roll axis and changes in spacecraft velocity. The thrusters also provide the capability to reduce the momentum stored in the reaction wheels. The reaction wheels have functional redundancy via a spare wheel oriented in a skewed position thereby providing a control component in all three axis. The thruster configuration provides functional redundancy.

The position of the high gain antenna and solar array are controlled via the electrical power subsystem.

### Mechanisms

The mechanisms on Odyssey provides the ability to restrain through the launch environment and then release the solar array, high gain antenna, and the Gamma Ray Spectrometer boom; the two axis gimbals to control the solar array and high gain antenna; the positioning of the Gamma Ray Spectrometer to a near and extended position.

The solar array is restrained by separation nuts. Upon release of the nuts, springs energy is used to provide the rotational

motion of the panels about their hinges. Dampers limit the rate of deployment. At full deployment the hinges latch into final position.

The high gain antenna is restrained by separation nuts. After release of the nuts the antenna boom initial motion is provided by spring energy, the subsequent rotation is provided by a redundant stepper motor/gearbox within the deployment hinge.

The two axis gimbals control the pointing on the solar array and high gain antenna. These gimbals utilize redundant stepper motors and position encoder electronics.

The Gamma Ray Spectrometer boom is restrained by a latch, which is released by the stroke of a high force thermal actuator. The thermal actuator uses a low melting point solder to achieve actuating force. After release, the boom deployment is driven by spring force; the deployment speed is limited by an eddy current damper, working through a gearbox and connected via a tether to the end of the boom.

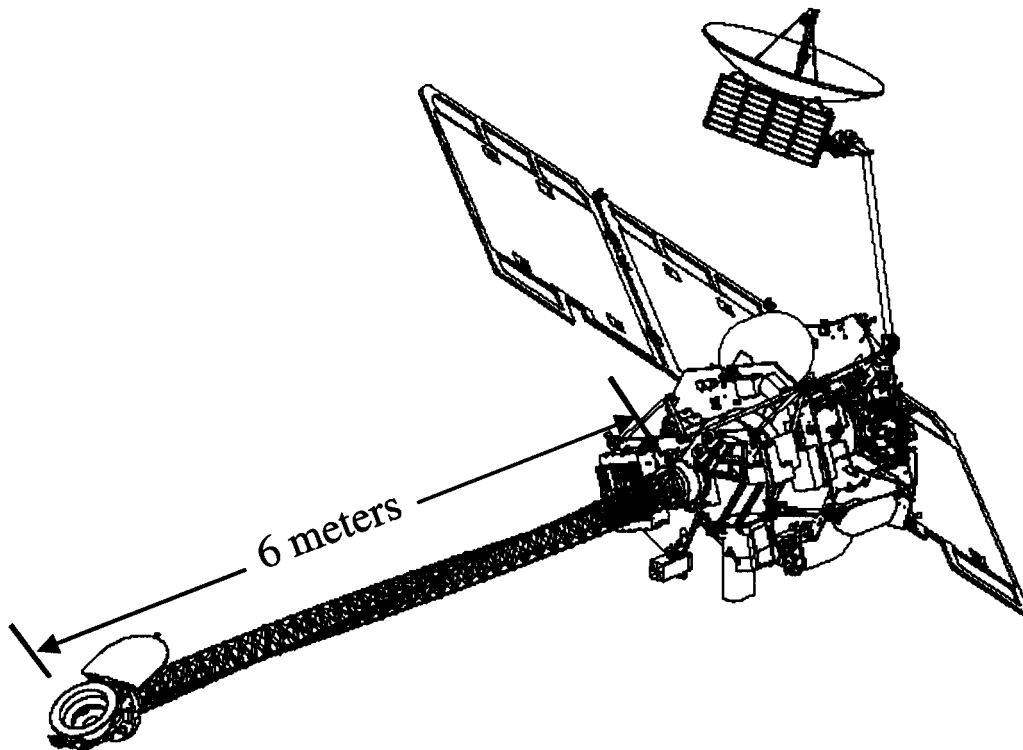


Figure 5. Gamma Ray Spectrometer Boom Deployed

## Propulsion

The propulsion subsystem provides changes to the spacecraft velocity on the trajectory to Mars, reduces the differential velocity between the spacecraft and Mars to allow the Mars gravitational field to capture the spacecraft in orbit, reduces (“unloads”) the momentum stored in the reaction wheels, and modifies the orbit characteristics during the orbital mission.

The spacecraft uses a dual fuel system, utilizing mono-methyl-hydrazine fuel and nitrogen tetroxide oxidizer. The main engine operates in a bi-propellant mode. The remaining thrusters use the fuel only in a mono-propellant mode.

The fuel tanks are symmetrically positioned to minimize changes in mass properties as the fuel and oxidizer are consumed during the mission. The fuel and oxidizer tanks are pressurized prior to launch. This initial pressure provides the required fuel flow for thruster operation during the cruise phase. A helium tank, operating through a pressure regulator, is isolated from the tanks until prior to the mars orbit insertion (MOI) maneuver. The helium tank provides a near constant pressure condition during the MOI maneuver; following MOI the helium pressure source is again isolated from the tanks. The spacecraft will operate for the remainder of the mission in a blow-down mode.

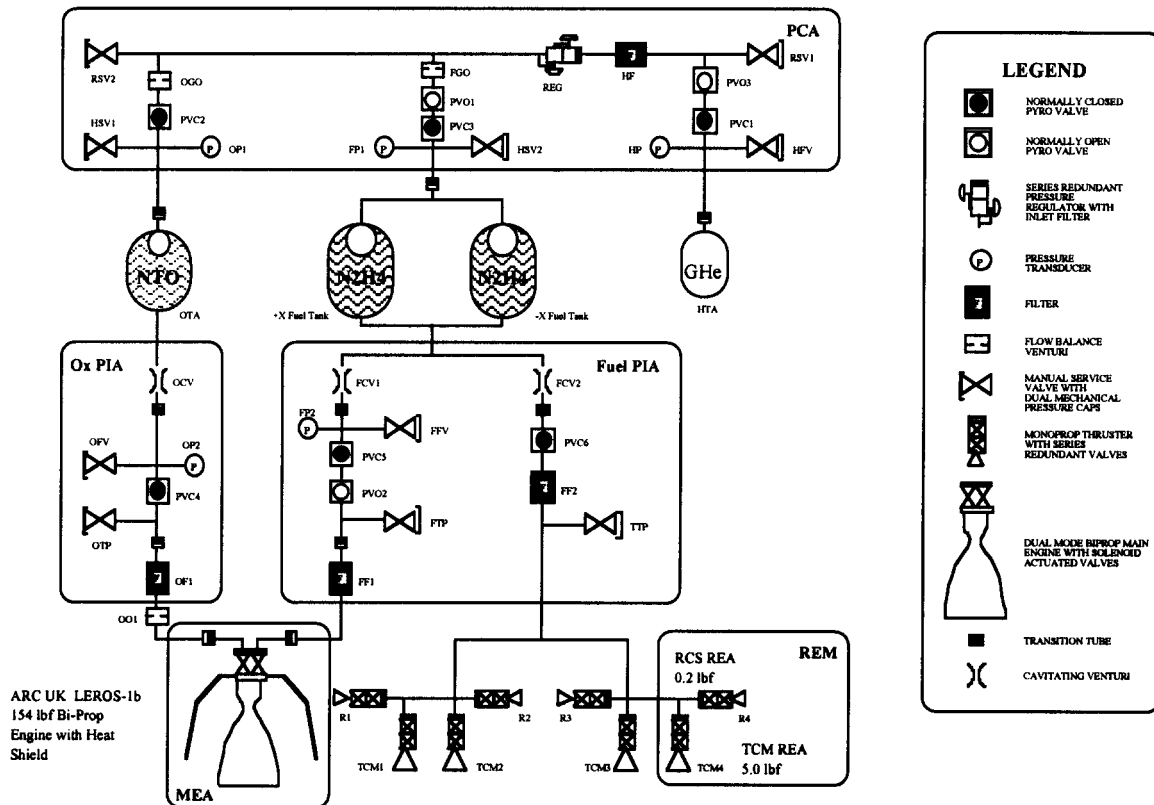


Figure 6: Propulsion Schematic

The main engine uses both hydrazine and nitrogen tetroxide and provides 695

Newtons thrust. The main engine is used only for the MOI maneuver, where it thrusts

for approximately 20 minutes. Following MOI the main engine and the nitrogen tetroxide tanks are isolated by valves for the remainder of the mission.

There are four rocket engine modules (REM). Each REM is comprised of a 0.9 N and a 22 N thruster. The 0.9 N thrusters provide roll control. The 22 N thrusters provide velocity changes and, during the MOI main engine operation, attitude control.

### **Software and Fault Protection**

The software stores the command sequence, executes the guidance, navigation and control functions, controls the science sensors, collects science data and spacecraft telemetry, and provides a data stream to the telecommunication subsystem for transmission.

The fault protection subsystem utilizes hardware and software sense and status data to assess hardware performance, detects loss of communication with ground operators, ensures spacecraft health and ability to receive commands from ground operators.

### **Structure and Harness**

The spacecraft structure provides a lightweight and rigid means of supporting the elements of the Odyssey and is designed and tested to withstand the loads of the launch environment.

There are two principle structural modules. The propulsion module contains the tanks, pressure regulator, filters, pyrotechnic valves, engines, and associated assemblies. The equipment module is composed of an equipment deck that supports engineering components and the radiation science experiment and the science deck that supports the thermal emission imaging system, gamma ray spectrometer, the high energy neutron detector, the neutron spectrometer and the star camera.

The structure is composed of composite construction techniques with metallic attachment points.

The harness provides the electrical routing of all power and data communication lines on the spacecraft.

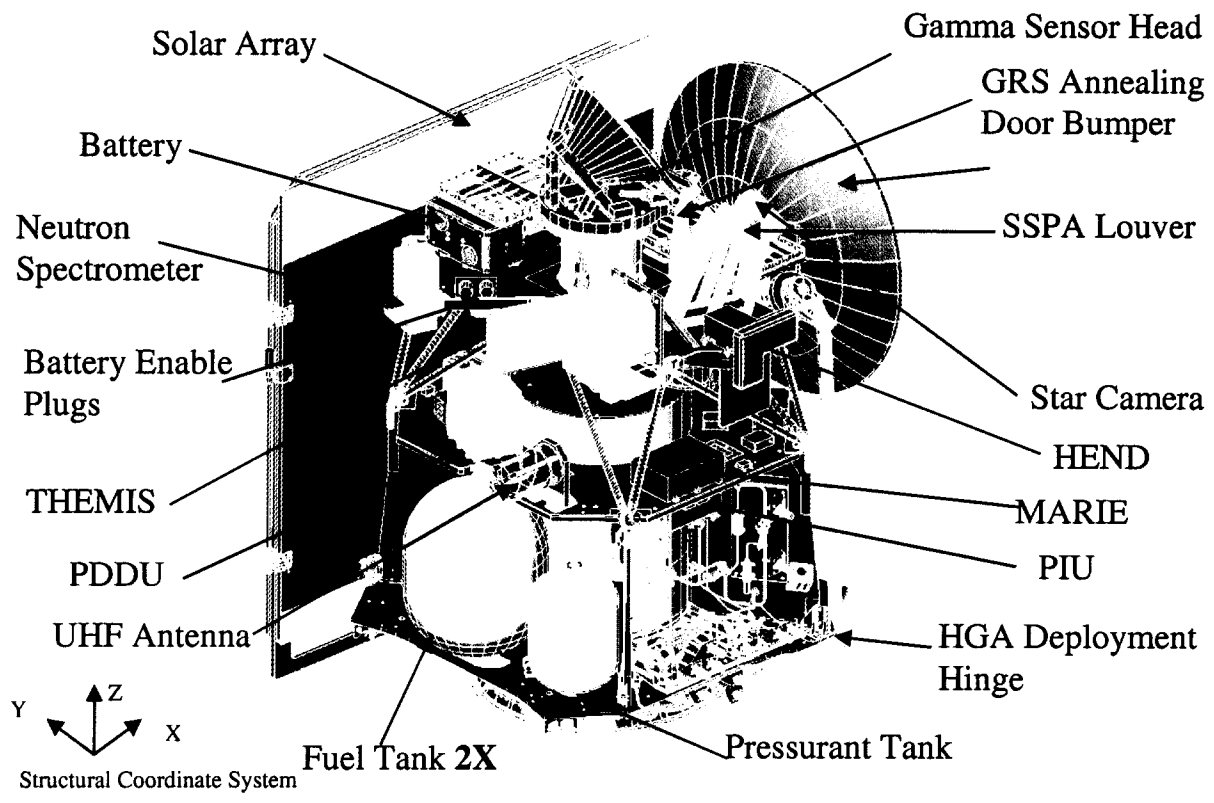


**Figure 7. Structure, Launch Configuration**

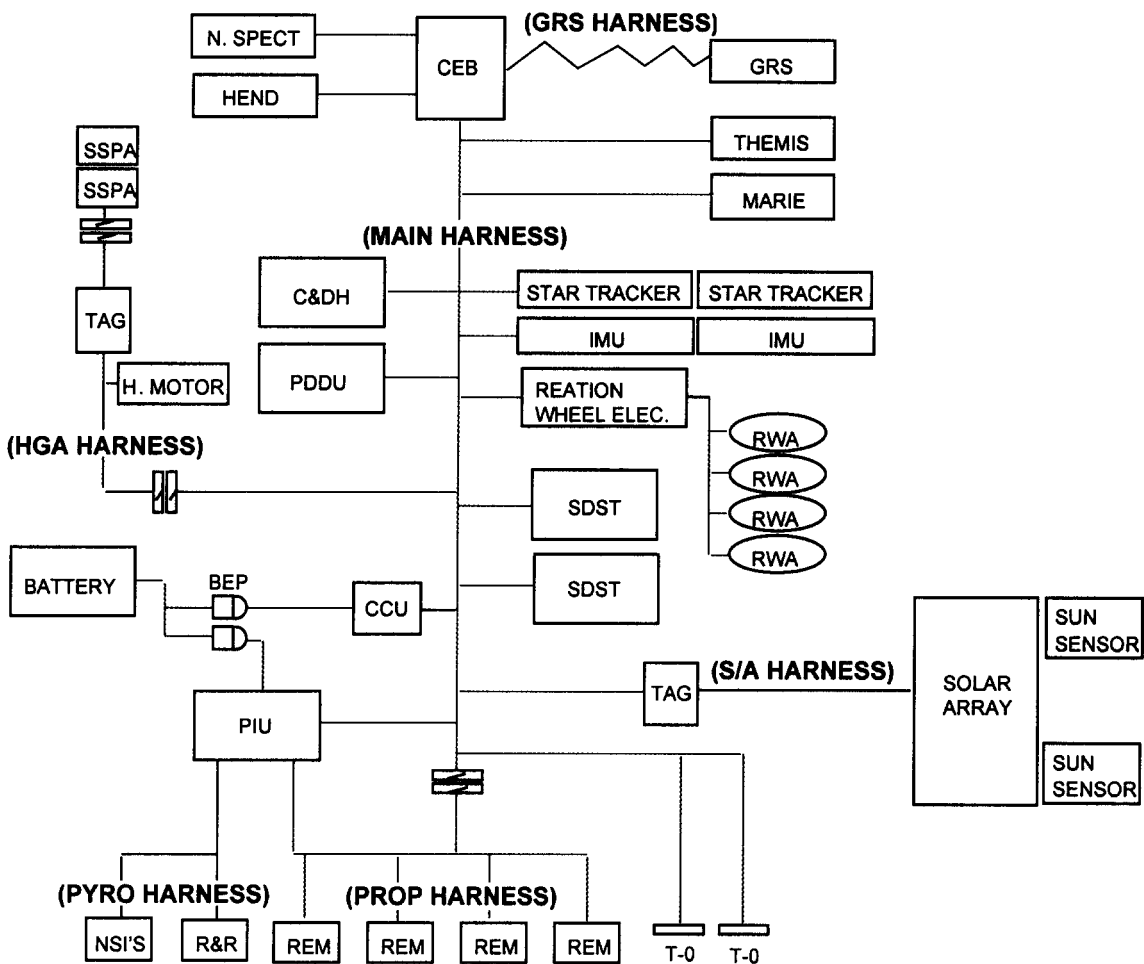


Figure 8. Harness Block Diagram

**Telecommunication**

The telecommunication subsystem is comprised of two separate radio systems. The X-band (4 GHz) radio system receives commands and data files from ground operators via the Deep Space Network (DSN), transmits data files to the ground operators via the DSN, and provides precise velocity and positional data via radiometric techniques. The UHF radio system (400 MHz) provides a radio relay capability between Odyssey and future assets at Mars, such as landers, rovers, or balloons.

The X-band system receives signals by either the highly directional high gain

antenna, or the wide coverage low gain antenna. Use of the parabolic 1.3 meter diameter high gain requires that the antenna actively tracks the Earth; the low gain 4.4 centimeter wide patch antenna allows communication over much greater spacecraft orientations.

The small deep space transponder (SDST) demodulates the RF signal and provides a symbol stream to the command and data handling subsystem for decoding. The SDST receives an encoded data stream from the command and data handling subsystem and provides a modulated, low level RF signal to the solid state power amplifier (SSPA). The SSPA amplifies this signal to

approximately 12 Watts. The amplified signal is then routed to either the high gain

or medium gain antenna for transmission to Earth.

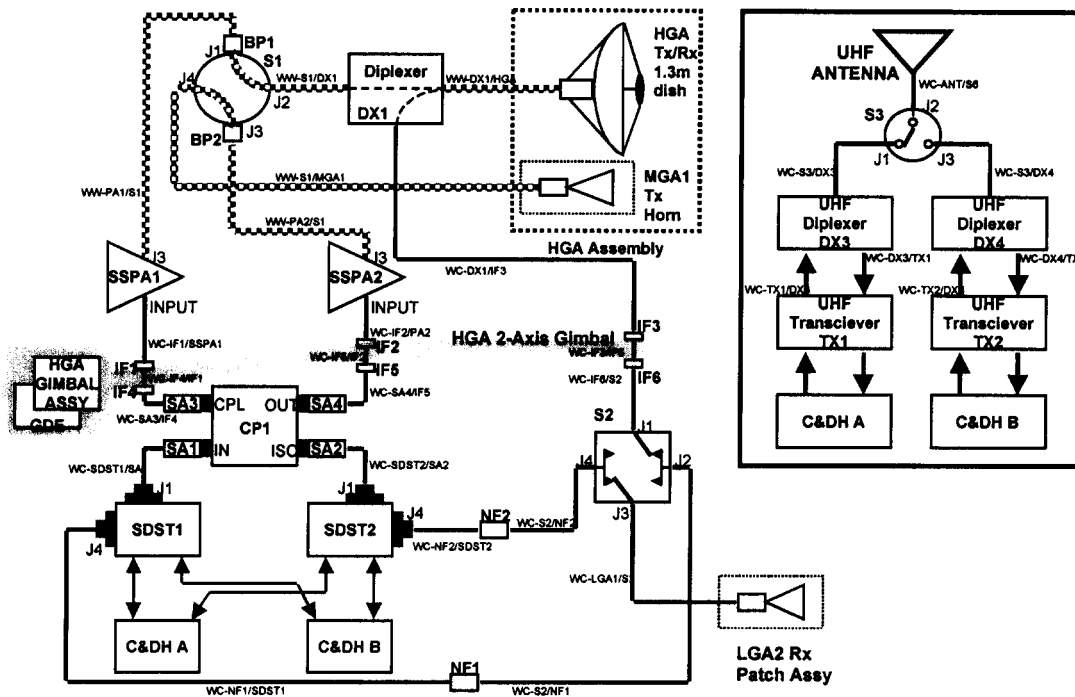


Figure 9. Telecom Block Diagram

### Thermal Control

The thermal control subsystem maintains the temperature of the spacecraft components within acceptable temperature limits through the range of mission phases, which include the near-Earth, interplanetary, and Mars orbit environments.

The spacecraft design uses a combination of passive and active means of thermal control. Multi-layer blankets limit the loss or absorption of heat energy by means of thermal radiation. Electrical heating elements are controlled by means of either mechanical switches or by software managed control. The solid state power amplifier and battery both utilize thermostatically controlled louvers for temperature control.

### Spacecraft Development Schedule

Following a 7 month Phase A study period, where initial requirements and capabilities were defined, the spacecraft design effort proceeded to Phase B. In Phase B, the system and science requirements were established, a technical baseline design and configuration were defined, orders were placed for long lead time parts, and the 11 month Phase B study concluded with a System Preliminary Design Review.

Phase C/D began October 12, 1998, approximately 31 months before launch. The System Critical Design review was held beginning on April 16, 1999. The Assembly, Test, and Launch Operations

began on January 18, 2000. The orbiter was air shipped to the launch site January 4, 2001. Final orbiter tests, instrument integration, spin balancing, fueling, and integration with the launch vehicle were achieved prior to launch.

### **Launch and Cruise Phase**

#### **Launch Phase**

Odyssey was launched from Space Launch Complex 17A (SLC-17A) at Cape Canaveral Air Force Station in Florida, on a Delta II in the 7925 configuration. The mission had designed a twenty-one day launch period that opened on April 7, 2001 and closed on April 27, 2001. There were two instantaneous launch opportunities each day corresponding to a launch azimuth of 65°, a long coast trajectory profile, and park orbit inclinations of 52° and 49°. The arrival date was dependent on the launch date, and Mars arrival was designed to occur between October 17 and October 28, 2001. Launch occurred on the first available opportunity, on the morning of April 7, 2001.

A typical Eastern Range flight profile was employed to achieve a 185 km circular parking orbit at the first cutoff of the second stage (SECO-1). Two plane-change (dogleg) maneuvers were employed to fly up

the coast of North America and achieve the desired parking orbit inclination. A thermal conditioning roll was employed during the coast period as the spacecraft flew over Europe, followed by the second stage restart. Over the Middle East, the third stage burn injected the upper stage/spacecraft stack onto the required escape trajectory, and after spinning up, the spacecraft separated nominally from the upper stage.

#### **Launch Targeting and Performance**

Planetary Protection policies require that, after injection, both the upper stage and the spacecraft must be on a trajectory biased away from Mars such that the probability of impacting Mars is less than 1 in 10,000. The size of the aimpoint bias is dependent on the expected injection dispersions. As propellant is required to correct for the bias, it is desirable to minimize the aimpoint correction.

The biased injection targets are expressed in terms of the energy (C3), declination (DLA), and right ascension (RLA) of the outgoing hyperbolic trajectory asymptote. The actual injection result can be compared against the target and expected dispersion statistics and presented as a sigma-level miss from the target:

Table 2. Injection Parameters

<b>Injection Parameter</b>	<b>Achieved</b>	<b>Delta from Target</b>	<b>Miss vs Expected</b>
<b>C3</b>	10.767	0.075	1.0 s
<b>DLA</b>	-51.669°	0.058°	1.0 s
<b>RLA</b>	235.169°	0.128°	0.3 s

The injection dispersions can be mapped along the nominal trajectory to the Mars target plane to illustrate the expected arrival conditions. The target and expected

dispersions are presented in Figure 10, along with the achieved. The launch dispersion happened to occur in a favorable direction.

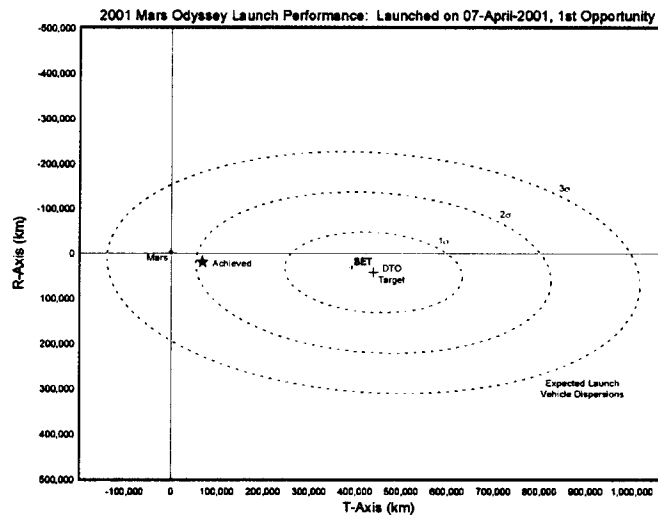


Figure 10. Odyssey Launch Performance

Following a successful separation from the launch vehicle upper stage, the spacecraft configured itself for the journey to Mars. The first activity was to deploy the solar arrays to begin recharging the onboard battery. Once the solar array was deployed, the attitude control subsystem performed a short series of Sun-search slew maneuvers to find the sun and to establish attitude reference. Once inertial attitude knowledge is established, with the solar arrays on the Sun, and the Medium-Gain antenna pointed at the Earth, communications with the spacecraft could begin.

The first DSN station to contact the spacecraft was DSS-34, the 34-meter Beam Wave Guide antenna at the Canberra, Australia complex, approximately 50 minutes after liftoff. Once initial contact was established, the command was sent to transition the telecom system to a two-way coherent mode of operation, to begin collection of Doppler and ranging data for Navigation purposes. The spacecraft was then commanded out of the planned launch safe-mode software state to the nominal

cruise attitude and flight software configuration. After several hours, the outer gimbal controlling the High-Gain Antenna, experienced higher than expected temperatures, so the spacecraft was returned from the cruise attitude back to the initial acquisition attitude. This marked the conclusion of the initial acquisition activities as the spacecraft proceeded with the planned cruise operations.

### Cruise Phase Overview

The relatively short interplanetary cruise phase of the mission lasted for 200 days. Activities during the cruise phase included initial deployments and checkout of the spacecraft in its cruise configuration, checkout and calibration of the spacecraft and payload subsystems, and navigation activities necessary to determine and correct the flight path to Mars.

Communication with the spacecraft is accomplished via the Deep Space Network (DSN) of ground-based radio antennas,

distributed around the world. Engineering telemetry, science data, and radiometric tracking data are collected during each tracking pass. One contact or *tracking pass* per day with a 34-meter antenna was standard for the cruise phase, with continuous tracking provided around the critical events such as launch, maneuvers, and final approach.

One peculiarity of the high negative declination trajectory is that for the first two months of cruise, only the southern hemisphere stations were able to view the spacecraft. During that time, the Canberra tracking stations had very long view periods, greater than 16 hours. Late in May, Goldstone came into view, and Madrid could not view the spacecraft until early June. A tracking station in Santiago, Chile was contracted to supplement the DSN for the first month of cruise.

The launch vehicle placed the spacecraft on a trajectory to Mars that did not require as much propellant as planned. So the first scheduled trajectory correction maneuver (TCM) at Launch+9 days (April 16) was delayed to Launch+46 days (May 23). The project realized a propellant savings due to the delay.

The first science instrument activity was an opportunity to image the Earth-Moon system with the THEMIS instrument. The instrument was powered on and performed a thermal calibration on April 17, ten days after launch, and successfully imaged the Earth and the Moon in a single frame in both the visible and infrared spectrums. On April 23 the MARIE instrument was powered on and began cruise science data collection.

Early attempts to transition the spacecraft to the desired cruise orientation, with the High Gain Antenna pointed at Earth, were aborted

due to higher than expected temperatures on the HGA outer gimbal. On April 24, as spacecraft attempted to transition to a modified cruise attitude that would shade the gimbal, the transition sequence was aborted by a safe-mode entry unrelated to the activity. The spacecraft memory had been corrupted by a high-energy particle, which resulted in a processor reset. Following the reset, the spacecraft entered safe mode, and the flight team quickly recovered to nominal mode, in the desired cruise attitude. For the remainder of cruise, the spacecraft was configured such that the stowed high-gain antenna pointed towards the Earth, and the solar array pointed generally towards the Sun with an offset angle profile.

The Neutron Spectrometer (NS) and High Energy Neutron Detector (HEND) were powered on as planned on May 2. On May 4 the first planned thruster calibration performed. A checkout of the High-Gain Antenna receive/transmit capability was performed on May 9, and on May 24 the communications path was switched from the LGA/MGA to the HGA to accommodate the increasing range of the spacecraft from the Earth.

The first trajectory correction maneuver executed nominally on May 23, firing the monopropellant TCM thrusters for 91 seconds. A test of the DOR tones in the Small Deep Space Transponder (SDST) was performed on May 24. And the first actual  $\Delta$ DOR (Delta-Differenced One-Way Ranging) measurement was performed on June 4, utilizing both the Goldstone, California and Canberra, Australia complexes. A total of 45  $\Delta$ DOR measurements were collected throughout the remainder of the cruise campaign.

Beginning on June 1, a series of tests of the UHF relay system were conducted with the

Stanford radio telescope. Ultimately three uplink/downlink tests were performed between June 6 and June 21 in addition to the initial compatibility test on June 1. A calibration of the solar array passive restraint was performed on June 20. This test involved articulating the solar array into and out of the restraint that would be used to hold it during the critical orbit insertion and aerobraking phases.

Following the development and uplink of a safe-mode patch to protect the GRS instrument, a low temperature anneal was performed on June 13. The GRS door was opened on June 25, and the high voltage ramped up two days later. The THEMIS instrument performed a visible exposure calibration on June 15 and a star calibration on June 22 to better characterize the instrument performance.

The second trajectory maneuver executed at 86 days past launch on July 2, and marked the transition from early cruise to late cruise. The mission plan had been designed to finish the majority of the checkout and calibrations prior to this time to provide a quiescent spacecraft in preparation for the coming arrival and orbit insertion events. However, a number of significant activities were executed in the final 114 days prior to encounter.

A follow-up calibration of the RCS thrusters was performed on August 8, followed two days later by a solar radiation pressure calibration. These tests were designed to ensure that the force modeling employed by the Navigation Team and the resultant trajectory perturbations were consistent with the spacecraft experience.

On August 13 communications was lost with the MARIE instrument as it hung in a transition from science mode to

survival/communications mode to download the collected data. A tiger-team was established to form a plan of action, and it became clear that the quickly approaching orbit insertion and aerobraking events would take a higher priority. So the ground analysis continued, but commanding to troubleshoot the anomaly was postponed until the completion of aerobraking.

The venting of the main engine in preparation for the large bi-propellant orbit insertion burn was performed on August 17. A test of the 110 kbps downlink data rate needed for THEMIS science operations was successfully demonstrated on August 24. Also in August, a series of Star Camera (SCAM) calibration tests were executed on the spacecraft. A number of star camera outages had been experienced throughout cruise when the SCAM was not explicitly shaded from the Sun by the HGA. It was also suspected that stray light from the open GRS door was saturating the SCAM images even when the SCAM was shaded by the HGA. The calibration confirmed that the orbit insertion and aerobraking attitudes would be safe, and that the closure of the GRS anneal door would resolve the issue for the remainder of cruise.

In preparation for final approach to Mars, the spacecraft instruments were turned off, and the spacecraft configured for arrival. The GRS door was closed on August 31, which was followed by a turn to the late cruise attitude on September 4. This late cruise configuration was designed to minimize the buildup of torque due to solar pressure effects on the offset solar array. And the final MOI checkout occurred on September 6.

The third trajectory correction maneuver executed on September 17, thirty-seven days prior to arrival. The HEND and NS were

turned off on September 24. The final trajectory correction maneuver executed on October 12, just twelve days prior to arrival. The operational MOI sequence was loaded onboard the spacecraft on September 15, nine days prior to MOI, and the spacecraft remained in a quiescent state for the remainder of the flight, until two days out when the solar array was stowed in preparation for the MOI burn. This activity marked the beginning of the MOI sequence of events.

### **Thruster Calibrations**

Reaction Wheel Assemblies (RWAs) provide primary attitude control and are desaturated by the RCS thrusters. This event, known as an angular momentum desaturation (AMD) is accomplished by firing the attitude control thrusters to unload the momentum. The thrusters fire in pairs to desaturate each spacecraft axis sequentially, but are not coupled. Desaturation events occurred on a daily basis throughout cruise. Because each thruster firing imparted a net change in velocity ( $\Delta V$ ) to the spacecraft, the thruster telemetry was recorded and downlinked for flight team evaluation. Although the net translational  $\Delta V$  from each event was small (less than 10 mm/sec) the cumulative trajectory perturbation was quite large, on the order of 10,000 km. So careful trending and calibration was required to meet the delivery accuracy requirements.

Two in-flight thruster calibration activities were performed. An *active* calibration occurred shortly after launch, which involved slewing the spacecraft to view the RCS thrusting from several different angles. Monitoring continued throughout cruise, and one *passive* calibration was performed which did not involve attitude changes.

The goal of the active calibration effort was to completely characterize the magnitude and direction of the thrust vector for each RCS thruster pair. The calibration was designed to fire thruster pairs in sequence to spin up, then spin down each reaction wheel. The translational velocity change was then measured with the Doppler, and the body and wheel rates were captured in telemetry. This sequence was performed in an Earth-pointed attitude, as well as three off-Earth attitudes. The combination provided a viewing profile that enabled the Doppler to sense the vector components of the velocity change from three nearly orthogonal attitudes.

The passive calibration was performed three months prior to encounter to ensure that the thruster behavior had not changed significantly. It involved all of the data collection, analysis, and interaction between the teams that was required for the active calibration, but did not involve any spacecraft attitude changes.

### **Trajectory Correction Maneuvers**

Although the ideal Orbiter trajectory does not require any deterministic deep space maneuvers to reach Mars, a schedule of four trajectory correction maneuvers (TCMs) was established to provide for sufficient control of the arrival conditions<sup>5</sup>.

TCM-1 was designed as part of a multi-maneuver optimization strategy to correct the injection errors, aimpoint bias and other trajectory errors while maintaining appropriate conditions for planetary protection. While the TCM-1 aimpoint is selected as part of the maneuver optimization strategy with some consideration for planetary protection requirements, the TCM-2 aimpoint was explicitly biased to satisfy overall planetary

protection requirements for the cruise phase. TCM-3 and TCM-4 corrected for the remaining trajectory errors and targeted directly to the desired encounter conditions in preparation for the Mars Orbit Insertion (MOI) burn.

All maneuvers were executed with the four 22 N TCM thrusters. In all cases, the  $\Delta V$  direction was constrained to ensure that the medium-gain antenna could maintain communications with Earth at the burn attitude. This constraint was incorporated into the aimpoint biases for the early

maneuvers to ensure a telecom link for TCMs 2 and 3. TCM-4 was a statistical *clean-up* maneuver, so could not be constrained a-priori, but a strategy was developed to maintain communications.

The  $\Delta V$  required for the cruise phase turned out to be substantially less than planned, again due to the positive injection results. The table below presents the planned (99%) and actual  $\Delta V$  and fuel usage associated with each maneuver, as well as the angle from the antenna boresight to the Earth.

Table 3. TCM Performance

<b>Planned Maneuver (99%)</b>	<b>Actual</b>	<b>Off-Earth</b>	
		<b>Fuel</b>	<b>Angle</b>
<b>TCM-1</b>	48 m/s	3.6 m/s	1.2 kg 7°
<b>TCM-2</b>	38 m/s	0.9 m/s	0.3 kg 14°
<b>TCM-3</b>	3.5 m/s	0.45 m/s	0.15 kg 2°
<b>TCM-4</b>	0.5 m/s	0.08 m/s	0.04 kg 20°
<b>Total</b>	<b>53 m/s</b>	<b>5 m/s</b>	<b>1.7 kg</b>

The total propellant budget for the cruise phase was dominated by the anticipated maneuvers, but it also included fuel allocations for momentum management, as well as for specific events and contingency. Of the total cruise allocation of 21.9 kg, only 3 kg were actually spent. This windfall was recognized shortly after launch, and the unspent fuel was termed *strategic propellant*, as the project then had the decision of how best to utilize this propellant to mitigate risk, modify the science strategy, or potentially extend the mission. The allocation of strategic propellant was an ongoing analysis that continued throughout the cruise and aerobraking phases.

### Delivery Accuracy

The primary navigation responsibility during the cruise phase was to accurately determine and control the trajectory of the spacecraft to deliver it to the desired aimpoint at Mars encounter<sup>6</sup>. This was accomplished by tracking the spacecraft radio signal to determine the orbit and designing propulsive maneuvers to alter the trajectory. Four maneuvers were scheduled to achieve the necessary delivery accuracy, with a fifth maneuver as a contingency in the final hours prior to encounter.

Although standard radiometric orbit determination techniques were employed to navigate the spacecraft, the traditional Doppler and ranging measurements were supplemented by a series of interferometric measurements known as delta-differenced

one-way ranging ( $\Delta$ DOR). This measurement is independent of the traditional radiometric measurements, and provides crucial *out-of-plane* trajectory information that is difficult to determine from more traditional data types. This technique has been utilized with success in the past, but the aging hardware and software system was completely re-built in preparation for this mission. A total of 45  $\Delta$ DOR measurements were planned and obtained over a five-month period.

The  $3\sigma$  delivery requirements were to meet the targeted altitude to within  $\pm 25$  km, the targeted inclination to within  $0.2^\circ$ , and the closest approach time to within  $\pm 10$  seconds. The table below presents the target and achieved values and demonstrates that the requirements were met. Figure 11 illustrates the target, the constraints and the actual delivery resulting from TCM-4. The final  $0.08$  m/s maneuver was designed to correct the residual targeting error left after TCM-3.

Table 4. Delivery Accuracy

<b>Parameter</b>	<b>Target</b>	<b>Achieved</b>	<b>Delta</b>
<b>Altitude</b>	300.0 km	300.7 km	0.7 km
<b>Inclination</b>	$93.47^\circ$	$93.51^\circ$	$0.04^\circ$
<b>Periapsis Time (ET)</b>	02:29:58	02:29:58	< 1 sec

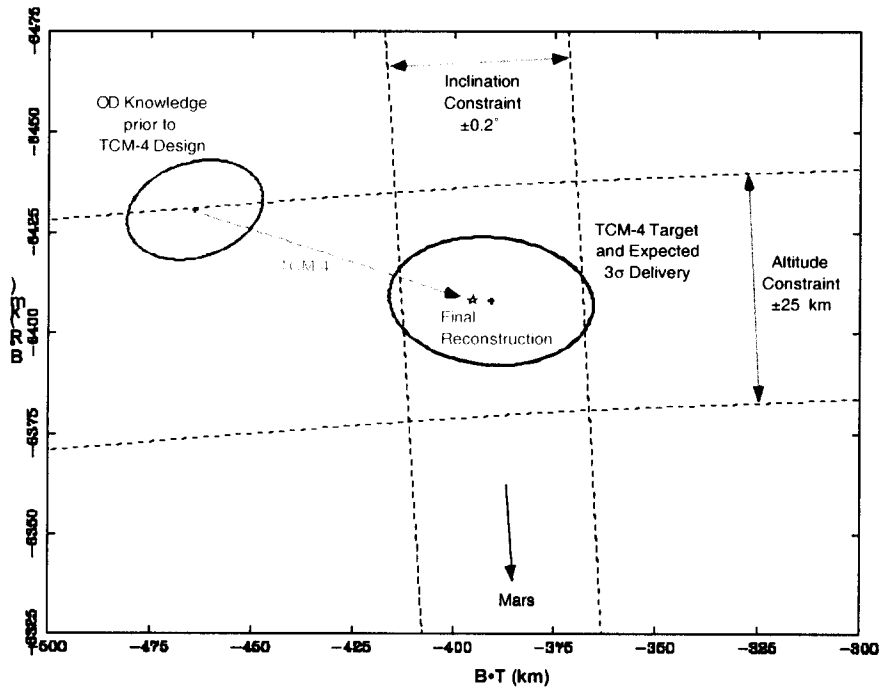


Figure 11. Final Delivery Accuracy

## Orbit Insertion Phase

Orbit Insertion phase began with the initiation of the Mars Orbit Insertion (MOI) sequence, nine days prior to encounter. At two days out, the solar array was stowed to configure the spacecraft for the MOI burn. The final TCM-5 maneuver opportunities at 24 hours, and six hours prior to MOI were not needed, and fault-protection was disabled at 22 hours out. Fifteen minutes prior to the start of the burn, the engine was filled, and shortly thereafter, the fuel and oxidizer tanks were pressurized. Seven minutes prior to the burn, the spacecraft slewed to the pre-burn attitude, and at this point could only communicate via the MGA in a carrier-only configuration. The main engine valves were opened simultaneously

at 02:26:57 UTC on October 24 to initiate the Mars Orbit Insertion burn, and the engine fired for just over twenty minutes. Throughout the burn, the spacecraft maintained a constant angular rate, termed a *pitchover*, to increase the efficiency of the capture maneuver. Ten minutes into the burn, the spacecraft passed behind Mars, as viewed from the Earth, and communications ceased as planned. The burn terminated when the on-board accelerometers detected a 15% thrust decay, indicating that the oxidizer had been depleted. Pyros were then fired to permanently isolate the pressurant from the propellant tanks. Ten minutes after the end of the burn, the spacecraft came back into view of the Earth, and communications was re-established.

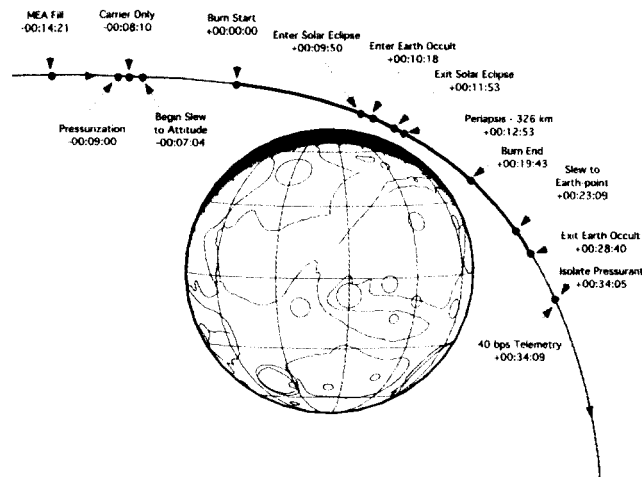


Figure 12. Mars Orbit Insertion

The nominal main engine thrust of 703 N, and Isp of 322.4 sec, along with the 121.3 kg of available oxidizer, defined the expected MOI burn time of 1183 seconds, expected total propellant expenditure of 266 kg, and  $\Delta V$  of 1420 m/s. Min and Max timers were set at 1115 and 1225 seconds respectively to ensure proper burn termination in the event

that the accelerometer did not accurately sense the depletion event.

The post-maneuver analysis indicated that the main engine burned for 1219 seconds, expended 146.3 kg of fuel, 121.4 kg of oxidizer, and produced a total  $\Delta V$  of 1433.1 m/s.

Based on statistics associated with the main engine performance, expected RCS performance during the burn, and spacecraft mass properties, the capture orbit period was expected to be 19 hours  $\pm$ 5 hours. Based on the planned aerobrake profiles and constraints, the project was able to define a maximum capture orbit period of 22 hours from which aerobraking could be safely initiated. If the capture orbit period exceeded this value, then a Period Reduction Maneuver (PRM) would need to be executed prior to the initiation of aerobraking to reduce the orbit period to an acceptable level. If needed, the Period Reduction Maneuver (PRM) would have executed about 48 hours after MOI in mono-propellant mode on the TCM thrusters. However, the achieved capture orbit period was determined to be below the mean at 18.6 hours and eliminated the need for a period reduction maneuver.

One other event that was closely monitored in the orbit insertion phase was potential close approaches with Phobos, the inner moon of Mars. The elliptical, polar capture orbit would permit close encounters with Phobos for particular capture orbit periods. Fortunately, the 18.6-hour capture orbit was out of phase with Phobos, and no collision avoidance maneuvers were necessary.

### **Aerobraking Phase**

The aerobraking phase began just two days after orbit insertion. Over the next three months, a total of 332 passes through the Martian atmosphere slowed the vehicle, reducing the orbit period to just under 2 hours<sup>6</sup>. The aerobraking phase required 24-hour per day operations at both JPL and LMA and daily support of teams across the country.

The aerobraking campaign was subdivided into three phases. The *Walk-In* phase gradually lowered the periapsis altitude from the 300 km capture orbit altitude down to the 110 km altitude desired to initiate main-phase aerobraking. *Main-Phase* constituted the bulk of the aerobraking mission both in terms of time, and number of drag passes. The aerobraking rate was determined by the heat rate corridor, and the bulk of the period reduction took place during this phase. As apoapsis decays, the aerobraking rate is eventually constrained by orbit lifetime. Lifetime in this context is defined to be the time it takes for apoapsis to decay to 300 km. Below this altitude, the orbit will degrade and the spacecraft will quickly spiral in. The *Walk-Out* phase of this mission was defined to occur when the orbit lifetime reached 24 hours.

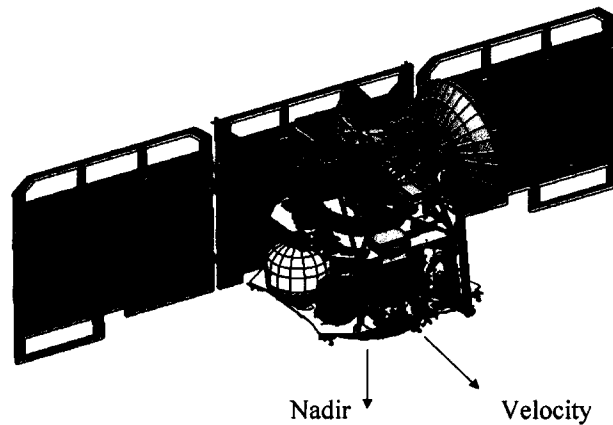


Figure 13. Odyssey Aerobraking Configuration

The dominant mission constraint throughout aerobraking was heating on the solar panels during the drag pass, which limited the total drag that could be achieved with each pass. On the other hand, a desire to limit the total number of drag passes, and a power constraint that limited the aerobraking duration, required that a minimum level of drag be attained in order to finish aerobraking successfully. These constraints were satisfied by instituting a range of acceptable heating rates (function of density and relative velocity) that were used to define the targeted aerobraking trajectory profile.

Energy balance was another key aerobraking constraint. As aerobraking progressed, the local true solar time (LTST) of the orbit decreased from at an average rate of ~2 minutes per day due to the motion of Mars about the Sun. As LTST decreases, solar occultation duration increases, reducing the power collection time to the arrays. A constraint was therefore imposed to maintain the LTST at the descending equator crossing to be later than 2 PM to 99% confidence to ensure adequate power to the spacecraft. This constraint effectively limited the aerobraking duration.

Variability of the Martian atmosphere significantly limited the ability to predict the density that would be observed on any given orbit. Overall, the observed variability exceeded 35% ( $1\sigma$ ), measured as the ratio of the heating rates on successive passes. To accommodate this uncertainty, 100% margin was generally maintained between the maximum targeted heating rate and the flight allowable limit. While this margin protected the vehicle from excessive heating, the uncertainty in the periapsis times that resulted from the limited prediction capability necessitated frequent updates to the on-board sequences.

### Spacecraft Operations

A number of spacecraft activities were required on each orbit to prepare the vehicle for the atmospheric conditions. Thirty minutes prior to the periapsis time, the catbed heaters were turned on to warm up the RCS thrusters, the solar array was articulated to the stowed position, communications was stopped as the SSPA was turned off, and the spacecraft would slew to the nadir-point attitude. At about five minutes prior to contact with the atmosphere, the attitude control mode was set to thruster control with loose deadbands.

As the spacecraft flew through the atmosphere, the atmospheric torque and attitude control thrusting would naturally desaturate the reaction wheels. One out of the atmosphere, the attitude deadbands were tightened, and control returned to the reaction wheels. The catbeds were turned off, and the spacecraft began its slew back to Earth-point attitude. Following the slew, communications was re-established as the SSPA was turned back on and the solar array was articulated out of the restraint and back to Sun-point. At this point the drag-pass telemetry playbacks and navigation tracking commenced. Two additional redundant telemetry playbacks were then scheduled in case the first was lost for any reason. Following the last playback, real-time telemetry was resumed until the next activity.

On selected orbits, the periapsis altitude was adjusted by performing an apoapsis maneuver. These aerobraking maneuvers (ABMs) were designed and built prior to MOI, and were designed to either raise or lower periapsis and to execute at apoapsis. So on ABM orbits, an additional sequence was built and uplinked. Twenty-five minutes prior to the apoapsis, the catbeds were turned on to warm up the TCM thrusters, the solar array was articulated to the stowed position, communications was stopped as the SSPA was turned off, and the spacecraft would slew to the burn attitude. The burn would initiate at apoapsis, followed by a slew back to Earth-point. The solar array was then deployed back to Sun-point, the SSPA turned back on to re-establish communications., and playback of the recorded ABM telemetry data commenced.

Drag sequences were generated and uplinked up to four times daily. The duration of each sequence was determined by the orbit period and the orbit timing prediction

accuracy. 225 seconds of timing margin was utilized to ensure that the spacecraft could transition into the proper configuration prior to and following each drag pass, and this drove the periapsis timing requirement. The sequence build schedule was driven by the ability to predict the upcoming periapsis times to within the 225 second requirement.

Atmospheric variability was the largest source of uncertainty in predicting the orbit timing. If the observed density for a given drag-pass did not match the predicted value, the amount of energy removed from the orbit, and therefore the period reduction achieved by the pass, would also not match the prediction. Thus, the time of the next periapsis would be different from the pre-pass prediction. If the periapsis timing error was determined to be greater than 225 seconds, the timing for the next sequence would need to be adjusted to reflect the new expected periapsis time.

Early in aerobraking, the nominal delta-period per orbit was more than 20 minutes, and the difference between the expected periapsis time and the actual time could easily be more than 225 seconds after only one pass; therefore, a new trajectory predict was delivered after every drag-pass to build the sequence for the upcoming pass. Later in aerobraking, as the nominal delta-period per orbit decreased, the error in the periapsis time prediction also decreased so that, gradually, more than one, and up to six orbits could be predicted within the 225 second constraint.

The Periapsis Timing Estimator (PTE) was an onboard software process that was designed to autonomously adjust the sequence timing based on the time that the drag-pass was sensed by the onboard accelerometers. This capability was successfully used to extend the peripaisis

timing prediction capability in the later phases of aerobraking when it was necessary to predict many orbits in the future.

It was at about the 9-hour orbit period when Odyssey began to experience unusually low atmospheric variability over the North Pole. We did not rely on this phenomenon ahead of time, but were able to take advantage of it in flight. The heat-rate upper corridor limit was effectively raised, and the aerobraking rate was increased for a time.

The Navigation timing and sequence build processes operated flawlessly throughout the aerobraking phase, and with the help of the Periapsis Timing Estimator (PTE) the orbit timing requirement was never exceeded. The daily strategic planning process also operated as planned, the flight allowable solar array temperature was never exceeded.

### **Transition to Mapping Orbit**

The transition phase was designed to provide the time required to perform the propulsive burns needed to achieve the final mapping orbit, deploy the high-gain antenna, and configure the spacecraft and the science payloads for mapping operations. The spacecraft was maintained in an inertially fixed, Earth-pointed attitude, with the solar array on the Sun for the majority of this phase. Momentum management was accommodated by angular momentum desaturations that occurred up to four times daily.

The primary navigation task during this phase was to design and execute the five transition maneuvers, beginning with the aerobraking termination maneuver, ABX1.

The ABX1 attitude was selected from a pre-designed menu that was used for all aerobraking maneuvers. The magnitude was

also pre-planned to be sufficiently large to raise periapsis altitude out of the atmosphere. The 20 m/s ABX1 maneuver executed on Apoapsis 336 on Jan 11, 2002, raised the periapsis altitude to 201 km, and marked a successful conclusion to the aerobraking phase.

The remaining maneuvers, although termed ABX2-5, were really orbit transition maneuvers. ABX2 was planned to execute several days after ABX1 at a time when the periapsis point had naturally drifted to the equator. At this time, it was optimal to perform a small inclination change, and raise the periapsis altitude again. The inclination change was designed to set up the desired Local Mean Solar Time (LMST) drift desired for the science orbit. ABX2 was the largest mono-propellant maneuver of the mission, and the 56 m/s maneuver was executed at apoapsis 393 on Jan 15, 2002. Following ABX2, the periapsis altitude was 419 km, and the inclination was 93.1°.

ABX3 was designed at the same time as ABX2, and was scheduled to execute just two days later to lower apoapsis and freeze the orbit. The frozen orbit condition requires the periapsis point to be at the South Pole, but at this time periapsis was still close to the Equator. The option to wait until periapsis naturally drifted to the South Pole was undesirable, as it would delay the start of the science mission by several weeks, and the natural eccentricity variation would require even more propellant to compensate. The 27 m/s ABX3 maneuver executed successfully on orbit 417 on Jan 17, 2002. This maneuver established the frozen orbit by rotating the periapsis point to the South Pole, and at the same time reducing the apoapsis altitude to 450 km, and periapsis to 387 km.

Following these large transition maneuvers, two orbit trim maneuvers were planned to clean up any residual orbit error. ABX 2 and 3 had executed just as planned, however, small execution errors and orbit propagation uncertainty left the need for some small clean-up maneuvers. A week of tracking and maneuver design was allocated, and the two trim burns ABX4 and ABX5 executed on Jan 28 and 30, 2002. The combined  $\Delta V$  of the two maneuvers was 3 m/s.

Once the propulsive maneuvers were completed, the high-gain antenna was successfully deployed on February 8, 2002. Several spacecraft and science payload housekeeping and checkout sequences were accommodated in the following weeks, and the spacecraft turned to nadir-point on February 18, 2002. The THEMIS instrument began imaging the planet on February 19, 2002, and the Gamma Ray Spectrometer began data collection, signaling the start of the 917-day science mission. In early March, the MARIE troubleshooting activity returned the radiation monitor to a fully operational state, resulting in a complete science payload complement for the science mission.

### **Science Orbit**

The science orbit was established on January 30, 2002 following the final transition orbit

trim maneuver. The 400 km, polar near-circular, frozen orbit provides the observational geometry desired by the science instruments. The orbit period of just less than 2 hours results in roughly 12.5 revolutions per Martian day, or sol. Successive ground tracks are separated in longitude at the equator by approximately  $28.8^\circ$  and the entire ground track pattern nearly repeats every 2 sols, with a  $1^\circ$  shift to the West.

The science orbit design was negotiated to balance the observational desires of THEMIS with those of GRS. The MARIE investigation is relatively insensitive to the orbit design. The somewhat conflicting requirements that drive the orbit design are that high-quality THEMIS infrared data are obtained at local true solar times (LTST) earlier than 5 PM, while GRS cooler constraints require solar beta angles less than  $-57.5^\circ$ . The LTST and beta angle profiles are controlled by the orbit inclination, which affects the orbit nodal precession rate, the rate at which the orbit plane rotates in inertial space. Figure 15 displays the time-history of the science orbit LTST and beta angle for the planned science mission. The figure also includes local mean solar time (LMST), and Mars to Earth range.

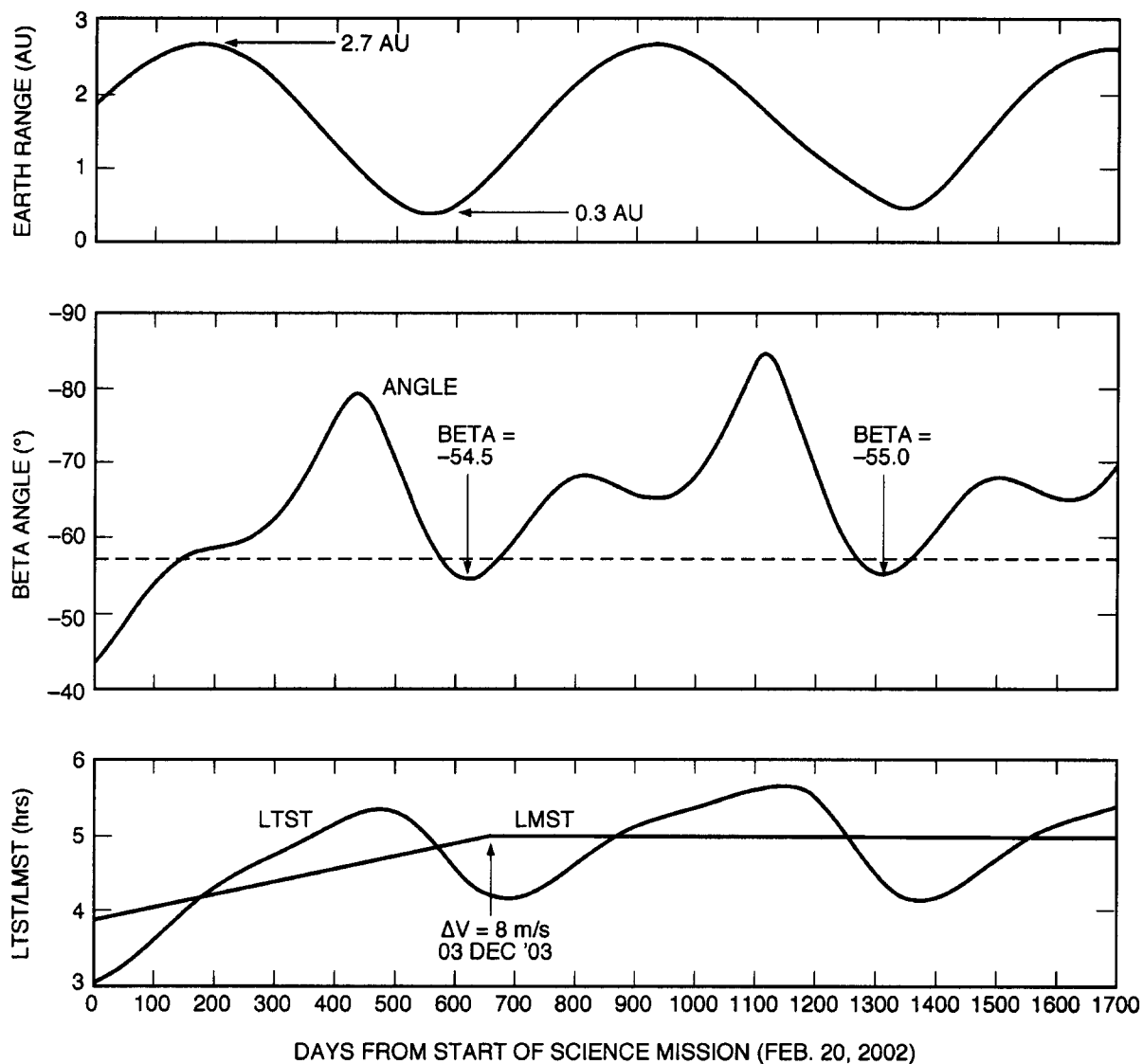


Figure 14. Science Orbit Geometry

The frozen orbit condition maintains a relatively fixed eccentricity and argument of periapsis for a given semi-major axis. The periapsis point is “frozen” at the South Pole, and the orbit altitude at any given latitude is constant at all longitudes. One key benefit of a frozen orbit for the Odyssey mission is that it keeps the Odyssey orbit away from the orbit of the Mars Global Surveyor, which is also in a similar frozen orbit.

Only two planned maneuvers remain during the mission. The first is a plane-change

maneuver to establish a Sun-synchronous orbit that would be desirable for an extended mission. The second is a planetary protection orbit raise maneuver that would occur at the end of mission. Propellant has also been allocated for any unplanned orbit trim maneuvers that may be required to compensate for the orbit perturbation from the desaturation events. Propellant for momentum management is required to maintain attitude and normal mapping operations. Contingency propellant has been allocated to accommodate off-nominal

operations, or safe-mode entries. The propellant budget was designed to provide a 99% probability of accommodating a 1374-day (2 Mars-year) mission. The propellant windfall continues, as a significant amount

of propellant remains unallocated. The detailed propellant allocations are shown in Table 5 (in kg, and equivalent  $\Delta V$ ).

Table 5. Science Mission Propellant Allocation

**Total Fuel Available:** 45.1 kg  $\pm$  3 kg (Mar 1, 2001)

<b>Allocations:</b>	<b>Fuel (kg)</b>	<b>DV (m/s)</b>
Contingency	8.2 kg	40 m/s
Safe Mode	5.0 kg	20 m/s
Momentum Mgmt.	11.5 kg	47 m/s
Orbit Trim Maneuvers	3.7 kg	18 m/s
Extended Science	1.9 kg	10 m/s
PQ Orbit Raise (EOM)	3.4 kg	18 m/s

**Unallocated Fuel Remaining:** 11.4 kg

### Science Mission

The 2001 Mars Odyssey mission contributes to the NASA Mars Exploration Program goals by a direct search for water in the near-surface of Mars at present and a search for evidence of past water in the surface mineralogy and morphology. In particular, 2001 Mars Odyssey carries instruments that will observe the Martian surface at infrared

and visual wavelengths to determine surface mineralogy and morphology, provide global gamma ray and neutron observations for a full Martian year, and study the Mars radiation environment from orbit.<sup>9-13</sup> The science payload on 2001 Mars Odyssey includes a gamma ray spectrometer, a multi-spectral thermal imager, and a radiation detector. An overview of these science instruments is given in Table 6.

Table 6. Science Payload Overview

Instrument	Description	Principal Investigator
THEMIS (Thermal Emission Imaging System)	Will determine the mineralogy of the Martian surface using multispectral, thermal-infrared images that have 9 spectral bands between 6.5 and 14.5 $\mu\text{m}$ . It will also acquire visible-light images with 18-m pixel resolution in either monochrome or color.	Philip Christensen, Arizona State University
GRS (Gamma Ray Spectrometer)	Will perform full-planet mapping of elemental abundance with an accuracy of 10% or better and a spatial resolution of about 300 km, by remote gamma ray spectroscopy, and full-planet mapping of the hydrogen (with depth of water inferred) and $\text{CO}_2$ abundances by remote neutron spectroscopy.	William Boynton, University of Arizona (GRS Team Leader, PI for Gamma Sensor)  William Feldman, Los Alamos National Laboratory (Neutron Spectrometer Scientist)  Igor Mitrofonov (High Energy Neutron Detector, PI)
MARIE (Martian Radiation Environment Experiment)	Will measure the accumulated absorbed dose and dose rate tissue as a function of time, determine the radiation quality factor, determine the energy deposition spectrum from 0.1 keV/ $\mu\text{m}$ to 1500 keV/ $\mu\text{m}$ , and separate the contribution of protons, neutrons, and HZE particles to these quantities.	Gautam Badhwar, Johnson Space Center (PI, deceased)  Cary Zeitlin, PI National SpaceBiomedical Research Institute Baylor University

### **Thermal Emission Imaging System (THEMIS)**

THEMIS addresses the Odyssey objectives of globally mapping the elemental composition of the surface, acquiring high spatial and spectral resolution images of the surface mineralogy, and providing information on the morphology of the Martian surface. THEMIS will characterize the Martian surface environment by providing high-spatial and high-spectral-resolution mineralogical and morphological data by means of visible and infrared imagery. Mineralogical and morphological measurements will help to determine a geologic record of past liquid environments. Furthermore, mineralogy and petrology data will help identify potential Mars landing sites. This experiment will provide essential information for selecting future landing sites aimed at exobiologic

exploration of Mars. Specific science objectives of the THEMIS experiment are to:

- 1) Determine the mineralogy and petrology of localized deposits associated with hydrothermal or sub-aqueous environments, and to identify sample return sites likely to represent these environments.
- 2) Provide a direct link to the global hyper-spectral mineral mapping from the Mars Global Surveyor (MGS) thermal emission spectrometer (TES) by utilizing the same infrared spectral region at high (100 in.) spatial resolution.
- 3) Study small-scale geologic processes and landing site characteristics using

morphologic and thermo-physical properties.

- 4 ) Search for pre-dawn thermal anomalies associated with active subsurface hydrothermal systems.

To accomplish these objectives, THEMIS will determine surface mineralogy using multispectral thermal-infrared images in 9 spectral bands from 6.5–14.5  $\mu\text{m}$  with 100-m pixel resolution. THEMIS will also acquire visible images at 18 m/pixel in up to 5 spectral bands for morphology studies and landing site selection. The THEMIS thermal-infrared spectral region contains the fundamental vibrational absorption bands that provide the most diagnostic information on mineral composition as all geologic materials, including carbonates, hydrothermal silica, sulfates, phosphates, hydroxides, silicates, and oxides have strong absorptions in the 6.5–14.5  $\mu\text{m}$  region. Thus, silica and carbonates, which are key diagnostic minerals in thermal spring deposits, will be readily identified using thermal-infrared spectra. Remote sensing studies of terrestrial surfaces, together with laboratory measurements, have demonstrated that 9 spectral bands are sufficient to detect minerals at abundances of 5–10%. The use of long wavelength infrared data has additional advantages over shorter-wavelength visible and near-infrared data because it can penetrate further through atmospheric dust and surface coatings, and the absorption bands are linearly proportional to mineral abundance even at very fine grain sizes.

THEMIS was designed as the follow-on to the Mars Global Surveyor Thermal Emission Spectrometer (TES), which produced a hyper-spectral (286-band) mineral map of the entire planet. THEMIS covers the same wavelength region as the TES, eliminating the need for additional

hyper-spectral mapping. Furthermore, the THEMIS filters were optimized utilizing knowledge of Martian surface minerals determined from TES data, and TES global maps will allow efficient targeting of areas with known concentrations of key minerals. Also, THEMIS will achieve infrared signal-to-noise ratios of 33 to 100 for surface temperatures (235–265 K) typical for Odyssey's mapping, ~4:30 p.m., orbit. In addition, this orbit is ideally suited to the search for pre-dawn temperature anomalies associated with active hydrothermal systems, if they exist. The visible imager will have a signal-to-noise ratio of greater than 100 at 5:00 p.m. local time. The THEMIS instrument weighs 10.7 kg, is 28 cm wide  $\times$  30 cm high  $\times$  31 cm long, and consumes an orbital average power of 5.1 W.

### **Gamma Ray Spectrometer (GRS) Suite**

The GRS instrument suite consists of three instruments including a gamma sensor head (GSH), a neutron spectrometer (NS), and a high-energy neutron detector (HEND). These instruments address the 2001 Mars Odyssey objectives of globally mapping the elemental composition of the surface, and of determining the abundance of hydrogen in the shallow subsurface. Thus, this instrument suite plays a lead role in determining the elemental makeup of the Martian surface

When exposed to cosmic rays, chemical elements in the Martian near-subsurface emit gamma rays with distinct energy levels. By measuring gamma rays coming from the Martian surface, it is possible to calculate surface elements' distributions and abundances. In addition, measuring neutrons provides a measurement of hydrogen abundance in the upper meter of

subsurface, which in turn provides inferences about the presence of near-surface water. Measuring neutrons also provides information about CO<sub>2</sub> abundances in the upper meter of subsurface.

The experimental objective of the GRS is to determine the elemental composition of Mars' surface by full-planet mapping of elemental abundance with an accuracy of 10% or better and a spatial resolution of about 300 km by remote gamma ray spectrometry, and full-planet mapping of the hydrogen (with depth of water inferred) and CO<sub>2</sub> abundances by remote neutron spectrometry. The instrument is also sensitive to gamma ray and particle fluxes from non-Martian sources and will be able to address problems of astrophysical interest including gamma ray bursts, the extragalactic background, and solar processes. The GRS principal investigator is Dr. William Boynton of the University of Arizona.

The GRS (as noted above) consists of several components. The GSH is separated from the rest of the spacecraft by a 6-m (20-ft) boom, which was extended after Odyssey entered its mapping orbit. This minimizes the interference from gamma rays coming from the spacecraft itself. The initial spectrometer activity, lasting about 100 days once the spacecraft was in its mapping orbit, provided instrument calibration before the boom was deployed. After about four months in the mapping orbit, the boom was deployed and it will remain in this position for the duration of the mission. The NS and the HEND components of the GRS are mounted on the main spacecraft structure and will operate continuously throughout the mission. The entire GRS instrument suite weighs 30.2 kg and uses 32 W of power. Along with its cooler, the GSH measures 46.8 cm long, 53.4 cm tall and 60.4 cm

wide. The NS is 17.3 cm long, 14.4 cm tall and 31.4 cm wide. The HEND measures 30.3 cm long, 24.8 cm tall and 24.2 cm wide. The instrument's central electronics box is 28.1 cm long, 24.3 cm tall and 23.4 cm wide.

#### *Gamma Sensor Head (GSH)*

The GSH will detect and count gamma rays emitted from the Martian surface. By associating the energy of gamma rays with known nuclear transitions and by determining the number of gamma rays emitted from a given portion of the Martian surface, it is possible to calculate the ratio of elemental abundances of the surface and discern their spatial distribution. While the energy represented in these emissions determines which elements are present, the intensity of the spectrum reveals the elements' concentrations. These energies will be collected with 600-km resolutions over time and used to build up a full-planet map of elemental abundances and their distributions. The GSH uses a high-purity germanium detector cooled below 100 K to measure gamma ray flux. GSH performance is a strong function of its temperature, which in turn constrains the spacecraft orbit beta angle (angle between orbit normal and direction to Sun) to insure that the GSH cooler is shaded from the Sun. The orbit beta angle must be less than  $-57.5^\circ$  ( $-56^\circ$  to shade the cooler plus pointing uncertainty of  $1.5^\circ$ ) in order to acquire useful data. Initial instrument calibration will be delayed until the beta angle geometry is satisfactory for GRS data acquisition. A periodic annealing of the germanium detector on the GRS may also be required. Each annealing cycle takes approximately 7 days.

#### *Neutron Spectrometer (NS)*

The NS measures neutrons liberated from the near-subsurface of Mars by cosmic rays.

Since Mars has a thin atmosphere and no global magnetic field, cosmic rays pass unhindered through the atmosphere and interact with the surface. Cosmic ray bombardment of nuclei of subsurface material down to about 3 m produces a large number of secondary neutrons. These neutrons in turn propagate through the subsurface and interact on the way out with subsurface nuclei. Fast neutrons produced by the cosmic rays may in turn be moderated by collisions with nuclei before they escape from the subsurface, resulting in neutrons with thermal or epithermal energies. The flux of secondary neutrons from the surface is the *neutron albedo* of Mars, which is measured by the NS. Goals of the NS are to:

- 1) Map the distribution of hydrogen within 1 m of the surface.
- 2) Map the seasonal variation of CO<sub>2</sub> ice and frost that forms on the polar caps during their winter seasons.
- 3) Map the major compositional provinces on Mars.
- 4) Provide maps of the neutron number density and fast-neutron flux at the surface of Mars for use in converting measured gamma-ray line strengths to elemental abundances.

The NS sensor consists of a cubical block of borated plastic scintillator that is segmented into four equal volume prisms. In the mapping orbit, one of the prisms faces forward into the spacecraft velocity vector, one faces backward, one faces down toward Mars, and one faces upward. Neutrons coming directly from Mars will be separated from those that are reprocessed by the spacecraft using a combination of velocity filtration (because the spacecraft in orbit about Mars travels faster than a thermal neutron) and self-shielding of one prism by the other three. Fast neutrons are separated from thermal and epithermal neutrons

electronically. Details of the instrument and the Doppler filter technique for separating thermal and epithermal neutrons have been given elsewhere<sup>14</sup>

The NS is provided and operated by the Los Alamos National Laboratory (LANL). William Feldman at LANL is the NS team leader within the GRS Team.

#### *High Energy Neutron Detector (HEND)*

The HEND complements the NS as it measures higher energy neutrons. HEND and NS together will map near-subsurface water and rock terrains. HEND consists of a set of five particle sensors and their electronics boards. The sensors include three proportional counters and a scintillation block with two scintillators. Proportional counters and an internal scintillator detect neutrons with different energies. When all these sensors are on, HEND measures neutrons over a broad energy range from 0.4 eV up to 10.0 MeV. HEND also helps calibration of the gamma sensor.

HEND will also provide astrophysical data about the nature of gamma-ray bursts and about the physics of solar activity. HEND data from extragalactic gamma ray bursts (GRBs) will be used with the data from Ulysses and near-Earth satellites (HETE-2, Wind, etc.). Interplanetary triangulation, a technique involving accurate timing of burst arrival times, allows the sky positions of the sources of GRBs to be determined with accuracy of several minutes of arc. HEND can also observe solar flares from different points in the Solar system. The simultaneous measurement of gamma rays and high-energy neutrons from powerful solar flares at Mars combined with those from the vicinity of Earth allows a stereoscopic image of the active region on

the Sun. These stereoscopic observations of powerful flares will provide the possibility to build a three-dimensional model of the generation of hard-electromagnetic radiation and corpuscular emission in active regions on the Sun.

HEND was developed in the Laboratory of Space Gamma Ray Spectroscopy at the Space Research Institute (Moscow, Russia). HEND is operated by the Russian Aviation and Space Agency's Space Research Institute in Moscow. Igor Mitrofonov is the principal investigator.

### **GRS Boom Deployment**

The GRS cooler door was closed on June 1, 2002, and the spacecraft slewed to the safe-mode (Earth-point) attitude on June 2, in preparation for GRS boom deployment. A GRS thermal control test and a demonstration of the control modes to be used during deployment were conducted on June 3. The boom deployment release mechanism was activated on June 4. The downlink signal from the spacecraft was lost shortly thereafter, as expected, due to the spacecraft motion induced by the boom deployment. Following rate damping and a slew back to Earth-point, high-rate downlink was reestablished, and engineering data for the deployment event was downlinked. Subsequent analysis indicated that the boom deployment was nominal, and the inertial measurement unit signature of the boom latching in its fully extended position was observed. Following boom deployment, the GRS cooler door was reopened, and the instrument high voltage was ramped up to begin science data collection.

### **Martian Radiation Environment Experiment (MARIE)**

The MARIE addresses the Odyssey objective of characterizing the Martian near-space radiation environment as related to radiation-induced risk to human explorers. As space radiation presents an extreme hazard to crews of interplanetary missions, MARIE's goal is to measure radiation doses that would be experienced by future astronauts and help determine possible effects of Martian radiation on human beings. Hazardous space radiation comes from two sources: energetic particles from the Sun and galactic cosmic rays from beyond our solar system. Both kinds of radiation can trigger cancer and damage the central nervous system. A spectrometer inside MARIE will measure the total energy from these radiation sources, both in cruise from Earth to Mars and in the Martian orbit. As the spacecraft orbits Mars, the spectrometer sweeps through the sky and measures the radiation field coming from different directions. Specifically, MARIE goals are to:

- 1) Characterize specific aspects of the Martian near-space radiation environment,
- 2) Characterize the surface radiation environment as related to radiation-induced risk to human exploration, and
- 3) Determine and model effects of the atmosphere on radiation doses observed on the surface.

The principal investigator for the MARIE experiment is Cary J. Zeitlin of the National Space Biomedical Research Institute at Baylor University in Houston. The MARIE instrument was provided by NASA's Human Exploration and Development of Space (HEDS) Program in order to

characterize the radiation environment at Mars. The instrument, with a 68-degree field of view, is designed to continuously collect data during Odyssey's cruise from Earth to Mars and in Mars orbit. It can store large amounts of data for downlink whenever possible, and will operate throughout the entire science mission. The instrument weighs 3.3 kg (7.3 lbs) and uses 7 W of power. It measures 29.4 cm (11.6 in) long, 23.2 cm (9.1 in) tall and 10.8 cm (4.3 in) wide.

### **Early Science Results**

The Odyssey science mission began on February 19, 2002, with the turn-on of the GRS instrument suite and THEMIS. MARIE began orbital science data collection on March 13, 2002. This section describes some science highlights from the first several months of the science mission.

### **GRS**

The GRS suite of instruments (HEND, NS and Gamma Sensor) was used to measure

and map hydrogen abundance in the upper ~ 1 m of the soil.<sup>15-17</sup> A strong signature of hydrogen was detected by all three sensors in the high southern latitudes, south of about 60° S. latitude. A deficit in the epithermal neutron flux, which is diagnostic of hydrogen, was mapped by both HEND and NS. Figure x is the epithermal neutron map obtained by NS from 30 days of mapping. A deficit in epithermal neutron flux is also observed in parts of the high northern latitudes, but most of the signature is likely masked by the cover of seasonal carbon dioxide frost in the north. The high flux of thermal neutrons seen by NS in the north is consistent with this interpretation.<sup>16</sup> By comparing the flux of epithermal and thermal neutrons, and the H gamma emission line observed by the gamma sensor, Boynton et al.,<sup>15</sup> were able to estimate the depth and quantity of hydrogen in the high southern latitudes. Model results suggest that the upper meter of the regolith contains a "dry" zone in the upper several 10s of cm, below which is an ice-rich zone with a mass fraction of water ice of 20-50%. Depth to the ice-rich zone decreases with distance to the south pole.



Figure 15: A global view of Mars in intermediate-energy, or epithermal, neutrons. Soil enriched by hydrogen is indicated by the deep blue colors on the map, which show a low intensity of epithermal neutrons. Progressively smaller amounts of hydrogen are shown in the colors light blue, green, yellow and red. The deep blue areas in the polar regions are believed to contain up to 50 percent water ice in the upper one meter (three feet) of the soil. Hydrogen in the far north is hidden at this time beneath a layer of carbon dioxide frost (dry ice). Light blue regions near the equator contain slightly enhanced near-surface hydrogen, which is most likely chemically or physically bound because water ice is not stable near the equator. The view shown here is a map of measurements made during the first three months of mapping using the neutron spectrometer instrument, part of the gamma ray spectrometer instrument suite. The central meridian in this projection is zero degrees longitude. Topographic features are superimposed on the map for geographic reference.

## **THEMIS**

Early THEMIS observations were targeted at high priority sites, including candidate landing sites for upcoming Mars lander missions. Data were acquired in all camera modes: day and night time infrared and day time visible. Performance of the camera system was excellent. Infrared images, both day and night, showed a remarkable diversity of temperature signatures of surface materials. Figure y is a mosaic of several day time single band infrared images near the hematite-rich candidate landing site in Terra Meridiani. Temperature variations in day time scenes result from differences in local slope relative to the sun, thermal inertia and albedo of surface materials. In the Meridiani image, variations in both thermal inertia and albedo cause strong contrast in temperatures, indicating differences in the physical properties of the layered materials currently exposed at the surface.

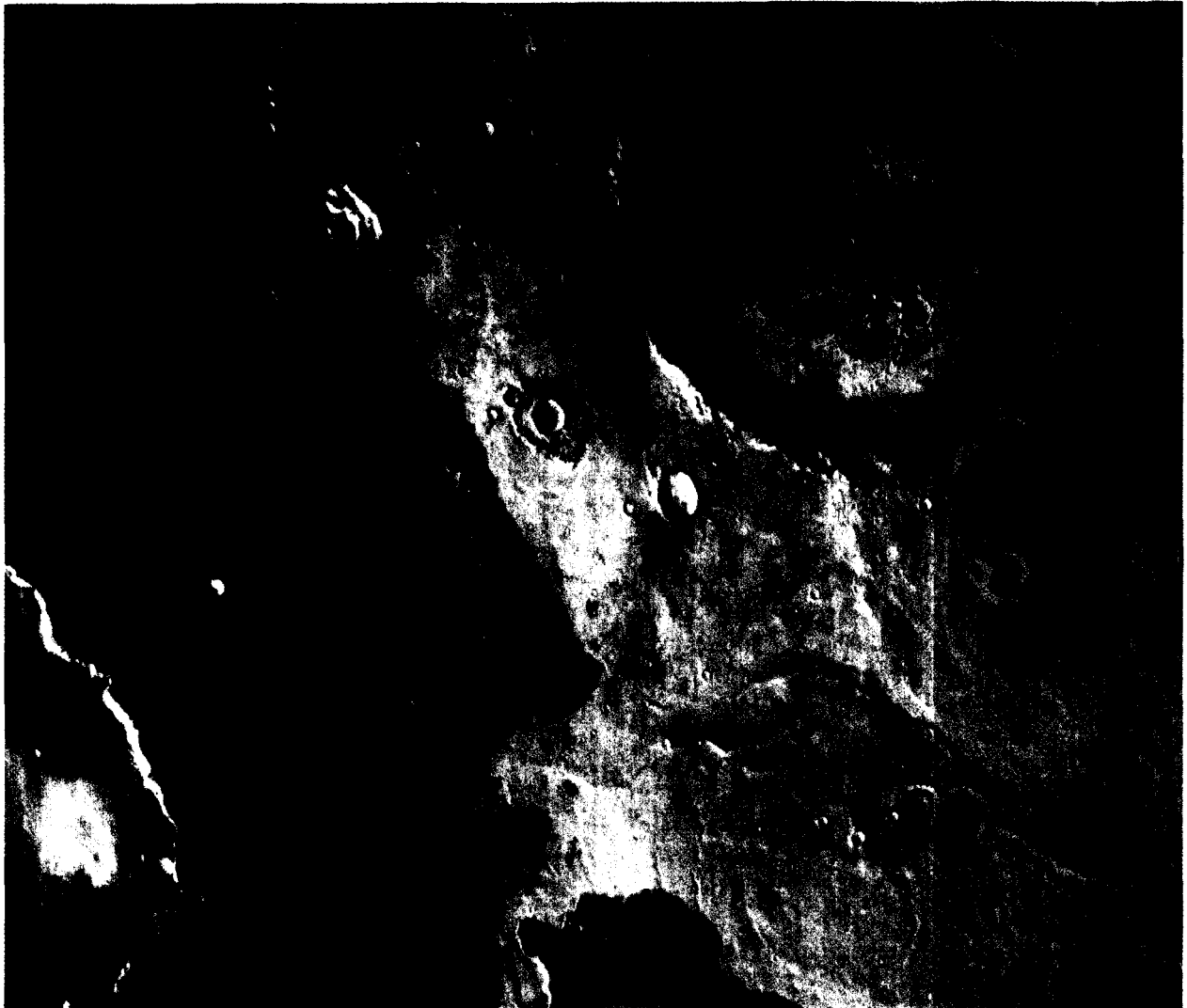


Figure 16: THEMIS infrared imaging shows signs of layering exposed at the surface in a region of Mars called Terra Meridiani. The brightness levels show daytime surface temperatures, which range from about minus 20 degrees to zero degrees Celsius (minus 4 degrees to 32 degrees Fahrenheit). Many of the temperature variations are due to slope effects, with sun-facing slopes warmer than shaded slopes. However, several rock layers can be seen to have distinctly different temperatures, indicating that physical properties vary from layer to layer. These differences suggest that the environment on this part of Mars varied through time as these layers were formed. The image is a mosaic combining four

exposures taken by the thermal emission imaging system aboard Odyssey during the first two months of the Odyssey mapping mission, which began in February 2002. The area shown is about 120 kilometers (75 miles) across, at approximately 358 degrees east (2 degrees west) longitude and 3 degrees north latitude.

Images from the THEMIS visible camera were published at the THEMIS website five days a week (<http://www.themis.asu>). Figure z is a single band visible image of another region in Terra Meridiani, showing heavily cratered terrain modified by channels and gullies.



Figure 17: A THEMIS visible image shows a region in Terra Meridiani near  $-12^{\circ}$  S,  $358^{\circ}$  W ( $2^{\circ}$  E). An old, heavily degraded channel can be seen from the lower (southern) portion of the image toward the top. The walls of several craters in this image show vague hints of possible gully formation at the bottom of pronounced rock layers, with the suggestion of alcoves above the individual gullies. Image size is 57.8 x 23.5 km.

### MARIE

Once nominal operation of MARIE was restored, the instrument collected radiation monitoring data nearly continuously. Figure 18 shows a sample of MARIE data collected during the first several weeks of operations. Radiation dose levels were close to those predicted from cosmic ray models. Solar activity was high during this time, which is reflected in the “spikes” of dose rate in the MARIE data.

### MARIE Measurements vs HZETRN Model Calculations

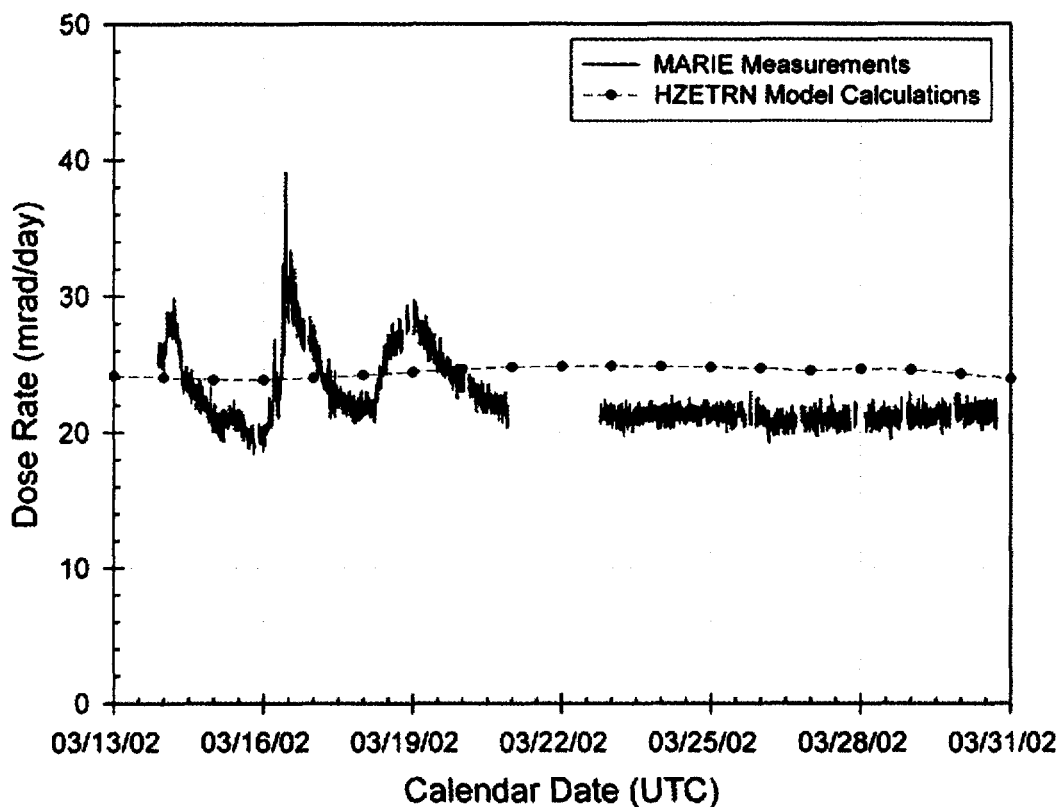


Figure 18: Absorbed dose rate as a function of time since MARIE was powered up in March. The gaps in data are related to downloads and housekeeping tasks. The solid line is the expected dose rate

calculated from the HZETRN model utilizing the daily solar deceleration parameter,  $\phi$  for the generation of the Galactic Cosmic Radiation spectra.

## **Risk Management**

### **Mission Fault Trees**

During the development phase, the project conducted a series of risk reviews to identify mission risk areas, and develop approaches for risk mitigation<sup>7</sup>. A working group comprised of systems, subsystems, operations, and the Assembly, Test and Launch Operations (ATLO) team was established to review each mission phase.

As part of the risk assessment, a fault tree was developed for each mission phase. The fault trees were used to identify what scenarios could lead to a mission failure, and to identify mitigations that prevent or reduce the probability of occurrence for that fault. It also listed how the mitigations were tested or analyzed. The fault tree is organized by function; in other words, it looks at what functionally needs to occur to achieve the objectives of that phase. It is complimentary to the System Failure Modes, Effects, and Criticality Assessment (FMECA) because it covers failures from functional viewpoint (e.g. what has to work) while the System FMECA lists how a specific component could fail (i.e. provides list of failure modes to feed into fault tree). The fault tree contains a verification table listing each fault in the tree, how the project is mitigating that fault, and where that mitigation is verified.

### **Contingency Planning**

The faults identified in the risk assessment were grouped into general categories, and then rated in terms of likelihood of occurrence, impact on the mission, and required recovery time. These ratings determine the category of the risks; contingency plans are developed according to the risk category. Category A mission

risks have significant mission impact and require quick turnaround; on-the-shelf commands are built and formal contingency procedures are developed for Category A risks. Category B risks do not require quick turnaround; informal procedures were written to serve as a reference for these contingencies. Category C risks are not mission critical, and are tracked without written response plans.

### **Risk Reduction Testing**

The Odyssey team instituted a program of testing called “risk reduction testing” or “flight software stress testing”. This test program augmented the project verification and validation process. Risk reduction testing began during the development program, and has continued through operations.

Key characteristics of the risk reduction test program include:

- 1) Focus on software performance in off nominal conditions.
- 2) Core team is independent of project software development and acceptance test team and project verification and validation test team.
- 3) Multiple combinations of failures, under-performing hardware, and fault protection cases are included in test cases.
- 4) Mindset of test case definition is “find a way to break it”, initial conditions allowed to go beyond specification limits.
- 5) Review of test case results performed by the main-line development and V&V team.

- 6) Results of test cases tracked by a formal action item/failure reporting system.
- 7) Schedule progress tracked and managed via an earned value system.
- 8) Test cases segregated by critical mission phases.
- 9) The suite of risk reduction testing was run on three test-beds – desktop software simulators, a high fidelity spacecraft simulator, and the flight vehicle on an approximate ratio of 100:10:1 .

The risk reduction test program differs from the software acceptance plan or the project verification and validation plan. The latter primarily verify that the system is designed to specifications and requirements and that the specifications and requirements are appropriate and sufficient for the mission. Risk reduction testing is focused on the behavior of the spacecraft as a system when operating in both nominal and off nominal conditions.

The risk reduction process proved to be quite valuable to the Odyssey project. Susceptibilities were identified by the risk reduction team, which the project then alleviated. Risk reduction testing offers the capability to perform many combinations and permutations of spacecraft operation, even in the condition of multiple faults and/or degraded hardware performance. Ultimately, this resulted in an improved characterization of system level performance, allowing increased robustness and increased assurance of mission success.

## **Red Team Involvement**

About one year before launch a “Red Team” was formed to review the Odyssey project. The characteristics of a Red Team include:

- Complete independence from the Project and limited independence from the Jet Propulsion Laboratory.
- Membership drawn from JPL, other NASA Centers, federally funded research and development centers, industry, and Academia .
- Chartered to perform an independent, detailed, comprehensive assessment of the entire Odyssey project.
- Red Team report to identify risk areas and recommend risk mitigation actions to improve the prospect for mission success.
- Scope of review included the flight system (including subsystems), the Mission Operations System, and the science instruments.

The Red Team was divided into a lead position (non-JPL) with a JPL co-lead. Sixteen subteams were formed to penetrate specific functions of the Project. The subteams developed findings and risk items independent of the Red Team leads. Red Team lead and co-lead did not change findings nor risk ratings submitted by the subteams.

The Red team process was roughly divided into two phases. In phase one, the Red Team was presented with design information via a technical interchange with the project team. Follow-up actions were completed and the Red Team produced a preliminary findings report. The report categorized identified risks and rated them for mission consequence and likelihood of occurrence.

In phase two, the project worked the risk items reported to reduce the likelihood and/or the consequences of the identified risks. The project response varied with the particular concern. In some cases, the Red Team was provided with additional information, once the nature of the concern was understood. Other responses included changes to the design, changes to the sequence of events, additional qualification or characterization testing, or further analysis.

The first report identified 117 risk items. As the Project and Red Team worked to mitigate these risk items to low risk and/or low likelihood additional risk items were identified. All Project closures were submitted to the initiator of the risk item for concurrence. All risk items, except two, were eventually closed as low residual risk. The two exceptions were: 1) the level of fidelity of the test bed should be improved, and 2) the spacecraft should operate in a dual processor, hot back-up mode during the Mars orbit insertion maneuver. These two risk items were the subject of much discussion. Ultimately the Project, which considered these to be low risk, and the Red Team, which rated these as significant (medium or high) risk, agreed to disagree. The results were presented to Governing Program Management Council (GPMC). The GPMC concurred with the project's recommendation to accept the residual risk areas identified by the Red Team.

### **Critical Event Readiness Reviews**

The Project conducted a Critical Event Readiness Review (CERR) prior to all critical mission events in the operations phase. The critical events are:

- Mars Orbit Insertion and Aerobraking
- High Gain Antenna Deployment
- Transition to Science Mapping
- Gamma Ray Spectrometer Boom Deployment

The purpose of a CERR is to demonstrate that all preparation is completed and that the Project is ready to proceed with low risk. The independent review board membership draws from JPL, our industrial partner Lockheed Martin Astronautics, and Science members. The review board report is submitted to the project and to the GPMC, which authorizes the project to proceed with the critical event.

The CERR is a comprehensive review which addresses:

- Mission, spacecraft, and Mission Operations performance to date.
- Status of the Incident, surprise, and anomaly (ISA) formal reporting system, with particular emphasis on ISAs which may be relevant to the critical event.
- Status of relevant action items.
- Review of development issues, as required.
- Reporting of personnel staffing and transition plans
- Status of the operational sequences, design, liens, test status, approval status.
- Status of the contingency plans and discussion of robustness to faults.
- Test verification/validation performed, risk reduction test status.
- Red Team report, as required.
- Staffing and training report.
- Identification of on-call technical experts.
- Facilities report, including status of backup facilities.

- Operational freeze status.
- Work to go plans.
- Media and public outreach plans, as required.

The CERR is typically schedule 4 weeks prior to the event. The GPMC reviews the results of the CERR typically two weeks prior to the event. At this time all items were 100% closed. Ultimate authority to proceed with the critical events is given by the GPMC.

The Critical Events Readiness Review process provided a method to systematically assess the readiness of the Project and provided high value to the project and our sponsors.

### **Conclusion**

The process of developing the 2001 Mars Odyssey flight vehicle, launching and operating the system throughout cruise, aerobraking, and the science mission, and

### **References**

<sup>1</sup>*Mars Surveyor 2001 Project Policies*, JPL D-16091, October 2, 2000.

<sup>2</sup>*Mars Surveyor 2001 Mission Plan*, Revision B, JPL D-1303, August, 2000.

<sup>3</sup>Spencer, D., Bell, J., Beutelschies, G., Mase, R., Smith, J.C., *2001 Mars Odyssey Mission Design*, Paper No. AAS 01-391, AAS/AIAA Astrodynamics Specialists Conference, July 30-August 2, 2001, Quebec City, Quebec, Canada.

<sup>4</sup>*Mars Odyssey 2001 Baseline Reference Mission*, Rev. B, Doc. No. MSP01-99-0195, 30 March 2001.

managing risk along the way, has been a complex and arduous undertaking. The early science discoveries of the mission are a testament to the dedicated work of the distributed Odyssey team. The flight vehicle is in excellent operating condition, and is poised to provide a rich harvest of science data from Mars for many years to come.

### **Acknowledgements**

The work described in this paper was performed at the Jet Propulsion Laboratory, California Institute of Technology, under contract with NASA. The authors would like to acknowledge the contributions of the spacecraft team at Lockheed Martin Astronautics in Denver, Colorado, and the science investigation teams at the University of Arizona, Arizona State University, NASA Johnson Space Center, Los Alamos National Laboratory, and the Russian Space Institute.

<sup>5</sup>Mase, R., Antreasian, P., Bell, J., Martin-Mur, T., Smith, J.C., *The Mars Odyssey Navigation Experience*, to be presented at the AIAA/AAS Astrodynamics Specialists Conference, August 5-8, 2002, Monterey, California.

<sup>6</sup>Antreasian, P., et al, *2001 Mars Odyssey Orbit Determination During Interplanetary Cruise*, AIAA-2002-4531, AIAA/AAS Astrodynamics Specialist Conference, Monterey, California, 5-8 Aug 2002.

<sup>7</sup>Smith, J.C., Bell, J., *2001 Mars Odyssey Aerobraking*, to be presented at the AIAA/AAS Astrodynamics Specialists Conference, August 5-8, 2002, Monterey, California.

<sup>8</sup>Beutelschies, G., *"That One's Gotta Work" Mars Odyssey's use of a Fault Tree Driven*

*Risk Assessment Process*, presented at the IEEE Aerospace Conference, March 9-16, 2002, Big Sky, Montana.

<sup>9</sup>Saunders, R. S., 2000. *The Mars Surveyor Program - Planned Orbiter and Lander for 2001*, 31st Annual Lunar and Planetary Science Conference, March 13–17, 2000, Houston, Texas, abstract no. 1776.

<sup>10</sup>Saunders, R. S., 2001a. *2001 Mars Odyssey Mission Science*, American Geophysical Union, Fall Meeting 2001, abstract #P41A-08.

<sup>11</sup>Saunders, R. S., 2001b. *Odyssey at Mars - Cruise and Aerobraking Science Summary*, American Astronomical Society, DPS Meeting #33, #48.07.

<sup>12</sup>Saunders, R. S., and Meyer, M. A., 2001. *2001 Mars Odyssey: Geologic Questions for Global Geochemical and Mineralogical Mapping*, 32nd Annual Lunar and Planetary Science Conference, March 12–16, 2001, Houston, Texas, abstract no. 1945.

<sup>13</sup>Saunders, R. S., Ahlf, P. R., Arvidson, R. E., Badhwar, G., Boynton, W. V., Christensen, P. R., Friedman, L. D., Kaplan, D., Malin, M., Meloy, T., Meyer, M., Mitrofanov, I. G., Smith, P., Squyres, S. W., 1999. *Mars 2001 Mission: Science Overview*, 30th Annual Lunar and Planetary Science Conference, March 15–29, 1999, Houston, TX, abstract no. 1769.

<sup>14</sup>Feldman, W. C., Prettyman, T. H., Tokar, R. L., Boynton, W. V., Byrd, R. C., Fuller, K. R., Gasnault, O., Longmire, J. L., Olsher, R. H., Storms, S. A., Thornton, G. W., 2001. *The Fast Neutron Flux Spectrum Aboard Mars Odyssey During Cruise*, American Geophysical Union, Fall Meeting 2001, abstract #P42A-0550.

<sup>15</sup>Boynton, W.V., W. C. Feldman, S. W. Squyres, T. Prettyman, J. Brückner, L. G. Evans, R. C. Reedy, R. Starr, J. R. Arnold, D. M. Drake, P. A. J. Englert, A. E. Metzger, Igor Mitrofanov, J. I. Trombka, C. d'Uston, H. Wänke, O. Gasnault, D. K. Hamara, D. M. Janes, R. L. Marcialis, S. Maurice, I. Mikheeva, G. J. Taylor, R. Tokar, C. Shinohara, 2002. *Distribution of Hydrogen in the Near-surface of Mars: Evidence for Sub-surface Ice Deposits* *Science* 297: 81-85.

<sup>16</sup>Feldman, W.C., W. V. Boynton, R. L. Tokar, T. H. Prettyman, O. Gasnault, S. W. Squyres, R. C. Elphic, D. J. Lawrence, S. L. Lawson, S. Maurice, G. W. McKinney, K. R. Moore, R. C. Reedy, 2002. *Global Distribution of Neutrons from Mars: Results from Mars Odyssey*. *Science* 297: 75-78.

<sup>17</sup>Mitrofanov, I., D. Anfimov, A. Kozyrev, M. Litvak, A. Sanin, V. Tret'yakov, A. Krylov, V. Shvetsov, W. Boynton, C. Shinohara, D. Hamara, R. S. Saunders, 2002. *Maps of Subsurface Hydrogen from the High-Energy Neutron Detector*, *Mars Odyssey Science* 297: 78-81.